CHAPTER IV

BLENDS OF LOW-DENSITY POLYETHYLENE WITH NYLON COMPATIBILIZED WITH SODIUM-NEUTRALIZED CARBOXYLATE IONOMERS

ABSTRACT: An ethylene-methacrylic acid copolymer partially neutralized with sodium (Na-EMAA), was successfully applied to compatibilize nylon6 (Ny6) and low-density polyethylene (LDPE) blends. The phase morphology and thermal behavior of these blends were investigated over range of composition. It was found that the addition of small amounts (0.5 phr) of Na-EMAA improved the compatible of the Ny6/LDPE blends; the uniformity and the reduction of dispersed phase size was observed. TGA measurement demonstrated the synergistic effect of the thermal stability when Na-EMAA was added. DSC results of Ny6/Na-EMAA binary blends showed that with increasing Na-EMAA content, the crystallization temperature of Ny6 phase decreased, indicating that Na-EMAA retarded the crystallization of Ny6. Melting point depression was found in both the Ny6 and LDPE phases in the ternary blends, indicating that Na-EMAA interfered with the crystallization of both blends. From the results, it can be concluded that during melt blending chemical and/or physical reactions have taken place between Ny6 and Na-EMAA, which confirmed by Molau test. Compared to our previous work, the Na^+ carboxylate ionomers are a more effective compatibilizer than the Zn^{2+} ionomers; however the copolymer itself was different between the Na^+ and Zn^{2+} materials so the comparison between the two cations is a direct one. Still however, this work shows that sodium-neutralized materials do serve as effective compatibilizers for nylon and LDPE.

Keywords: Sodium-neutralized carboxylate, Ionomers blend, Compatibilizer, Low-density polyethylene, Nylon6

INTRODUCTION

Blending of polymers is an excellent way for developing new materials with improved properties. Most polymers are incompatible and various morphologies can be realized via melt processing, for instance droplets or fibers in a matrix as well as stratified or co-continuous structures. The structures induced are usually thermodynamically unstable, and the mechanical properties of the blends are poor because of poor adhesion between the phases.

Nylon (Ny) and polyethylene (PE) blends are thermodynamically immiscible and mechanically incompatible; however a compatible blend of the two components would possess interesting properties based on the complementary behavior of the individual components. A good example is food packaging, due to the good oxygen barrier, very high strength, and high heat resistance of the Ny and the excellent moisture barrier, good flexibility, ease of processing of the PE.[1] The morphology and the properties of the immiscible blends can be enhanced by adding a third component, an interfacially active polymer, called a compatibilizer, which promotes physical and/or chemical interactions between the components. The compatibilizer will typically either be a chemically modified ethylene homopolymer, i.e. via post-polymerization maleic anhydride grafting,[2, 3] or an ethylene copolymer, i.e. an ethylene-acrylic acid copolymer.[4-8]

The functionalization of polyethylene with a small amount of ionic groups is a particularly attractive way of compatibilizing nylon with polyethylene because the amide groups may interact with the ionic groups via hydrogen bonding, ion-dipole interactions or/and metal-ion coordination during melt blending.[9,10] The introduction of such specific interactions can improve compatibility and may promote miscibility of polyamide and polyethylene blend.[1, 11-15] Further, compatibility of Ny and PE blends has also been attributed to amidation reaction occurring between the terminal end groups of Ny and the carboxylic acid groups.[12] Copolymers of ethylene with monomers containing acid groups are important commercial products. These materials are sold commercially with either hydrogen as the neutralizing agent for the acid group, or with a metal cation as the neutralizing agent. The latter are termed ionomers, and typically the amount of acid groups neutralized with a metal cation is

less then stoichiometric. One common commercial type of ionomer is a copolymer of ethylene and methacrylic acid marketed by DuPont under the trademark Na-EMAA. The two most common neutralizing cations are zinc (Zn^{2+}) or sodium (Na^+). The properties of zinc-neutralized and sodium-neutralized carboxylate ionomers are very different, such as sodium ionomers absorb significantly more water and tend to have higher fractional crystallinities than zinc ionomers.

Zinc-neutralized ionomers have been studied as blend compatibilizers extensively. The impact resistance[3], tensile properties[1,11], and barrier properties[16] of Ny and PE blends showed marked improvement with the addition of compatibilizer. Thermal stability of Ny6 and PE blend observed by TGA technique can be improved by adding of acrylic acid onto PE[5], and the crystallization behavior of this blend were also observed by WAXS.[6,7] The Ny6 or LDPE crystallize into spherulites with dimension smaller than those of the corresponding neat polymers and crystallization temperature dramatically shifted toward lower temperatures. In this present work, blends of nylon 6 and low density polyethylene (LDPE), using sodium-neutralized copolymers of ethylene and methacrylic acid (Na-EMAA) as a compatibilizer, were produced. Blends of Ny6 and Na-EMAA, as well as Na-EMAA and LDPE, were also investigated. Attention was focused on the thermal behavior, crystalline structure, and phase morphology of these blends as a function of the compatibilizer content, and the effect of EMAA with different type of neutralizing metal ions on Ny6/LDPE blends were also investigated.

EXPERIMENTAL

Materials

Ultramid B3 Nylon 6 (density 1.31 g/cm^3) was supplied by BASF (Thailand) Co.,Ltd. Low-Density Polyethylene, LD 1450J, was an injection molding grade polymer (density 0.914 g/cm^3) graciously supplied by Thai Polyethylene Co.,Ltd. Sodium-neutralized poly(ethylene-co-methacrylic acid) ionomers marketed under the trademark Na-EMAA® 8527, which contain 10% acid content and 54% neutralization, (density 0.94 g/cm^3) was supplied by DuPont (USA).

Blends Preparation

Prior to blending, all the blend compositions were external mixed using a tumble mixer for 10 minutes followed by drying them under vacuum at 60°C for 24 hours. The materials were blended in a Collin D-8017 T-20 twin screw extruder using a screw speed of 40 rpm. The blends were extruded through a single strand die, the extrudates were cooled in a water bath, then dried at ambient temperature and pelletized.

Specimen Preparation

Test specimens were obtained using a Wabash compression press machine. The pellets were placed in a picture frame mold and preheated at 240°C for 3 minutes between the plates without any applied pressure to allow for complete melting. After this period, a pressure of 10 tons was applied at the same temperature for 3 minutes. The sample was then slowly cooled to 40°C under pressure. Test specimens were cut from the molded sheets using a pneumatic die cutter.

Scanning Electron Microscopic Analysis

The fracture micrographs as well as the dispersed structure of the fractured samples were studied using a scanning electron microscope, JEOL (MP 152001), operated at 15-25 kV. The samples fractured under liquid nitrogen and were also subjected to selective extraction of the LDPE and Na-EMAA ionomers phases by immersing in hot decalin for 15 minutes and by formic acid to remove the Ny6 phase. The specimens were then coated with gold under vacuum to make them electrically conductive. The number average diameter (d_n) was calculated using equation 1,

$$d_n = \Sigma(n_i d_i)/\Sigma n_i \qquad (1)$$

where; n_i is the number of droplet and d_i is the diameter of the ith droplet.

X-ray Diffraction Analysis

Wide angle X-ray diffraction (WAXS) investigations of the neat Ny6, LDPE, and Na-EMAA ionomers as well as their blends were carrier out at room temperature using a Rigaku Rint 2000 diffractometer equipped with a graphite monochromator

and a Cu tube for generating CuKα radiation (1.5046Å). The diffraction scans were collected between 2θ values of 5 and 40° using a scan speed of 5 °C/min, CuKα radiation (λ=0.514), at 40 kV and 30mA.

Thermogravimetric Analysis

A DuPont TGA 2950 thermogravimetric analyzer was used to collect thermogravimetric data. 10±0.5 mg samples were heated 30-600°C at three different heating rates of 10, 20, 40°C/min in a platinum pan under air.

Differential Scanning Calorimetry

Thermal analysis was carried out on a differential scanning calorimeter, Perkin-Elmer DSC 7. All the scans were made under nitrogen atmosphere to minimize oxidative degradation. The temperature calibration of the DSC was obtained by measuring the melting temperature of indium as a standard. 10 mg samples were encapsulated in an aluminum pan, heated from 25°C to 250°C at a heating rate of 80°C/min, held for 5 minutes at this temperature to remove their thermal history, followed by cooling to 30°C at 10°C/min. The crystallinity of the sample was also determined from a knowledge of the ratio of the melting enthalpy for 100% crystallinity of pure components. The absolute crystallinity of the blend was calculated using equation 2,

$$\chi_c = \frac{\Delta H \times 100\%}{\Delta H_f \times \text{wt.fraction}} \tag{2}$$

where; χ_c is the % weight fractional crystallinity, ΔH is the melting enthalpy of the component present in the blends, ΔH_f is the heat of fusion for the 100% crystallinity of the pure component, (190 J/g for Ny6, and 282 J/g for LDPE).[11]

RESULTS AND DISCUSSION

Scanning Electron Microscopy Analysis

SEM micrographs of compression molded samples after cryogenic fracture of Ny6/LDPE binary blends, i.e. a blend prepared without any compatibilizer, are

shown in Figure 1. The presence of a dispersed phase, consisting of predominantly spherical droplets imbedded in a matrix, is clearly observed from the micrographs of the whole composition range. As expected, the adhesion between the Ny6 phase and the LDPE phase is poor, as confirmed by the surfaces of the remaining holes appearing to be very smooth.[14] The d_n of the dispersed phase were determined for this blends, and the result shown in Table 1. The diameter of dispersed particles show in range between 13 to 26 μm, with an non-uniform morphology.

In order to better determine the morphology, micrographs are presented after the dispersed phase LDPE was extracted from the Ny6 matrix, i.e. 80/20 Ny6/LDPE blend in Figure 2. The addition of small quantities of Na-EMAA to Ny6/LDPE blends resulted in remarkable changes in the morphology. The particles of the dispersed phase become more uniform and much reduced in size presumably due to interactions between the ionomers and the Ny6. In fact, Figure 3 seems to show a coating on the surface of the dispersed particle. Macknight et al.[12] as well as others have suggested two possible specific interactions between nylon and the ionomer, first hydrogen bonding between the amide nitrogen on the nylon and the carboxylic acid on the ionomer, and second a covalent amide bond which can form between the primary amine at the end of the nylon chain and the carboxylic acid of the ionomer. Note that this material, as all commercial ionomers, was only partly neutralized with sodium; additional carboxylic acids are available for both these functions.

The dispersed particles were in range between 2-6 μm and were six times smaller than in the uncompatibilized blend. In Figure 3(b)-(d), they appear that only 0.5 phr of Na-EMAA is sufficient to produce a maximum reduction of the dispersed phase sizes. No further decrease in phase size is achieved by adding more Na-EMAA, as seen from the plateau region of the plots between average dispersed phase diameter and amount of Na-EMAA added shown in Figure 4. This is consistence to the result obtained for zinc ionomers of E-MAA employed previously.[14,15] The quick plateau presumably is due to a saturation effect at the interface coupled with the processing technique use, in other words 0.5 phr is all that is necessary to stabilize 2-6 μm particles. The twin-screw extruder is able to take the minor phase and reduce

individual domain sizes to 2-6 μm. The reduction in average droplet size is due to a suppression of coalescence; the compatibilizer has little effect on the extruder's ability to breakup molten polymers into smaller domain sizes.

The phase morphology of the Ny6/LDPE/ionomers blends were not depended only on the amount of Na-EMAA ionomers, but also on the type of metal cation of the ionomers. The average dispersed size of the blends compared between Na^+ and Zn^{2+} were shown in Table 1. The result clearly showed that Na^+ cation posses higher reduction of disperse size than Zn^{2+} neutralized Na-EMAA, suggesting that the interactions of Na^+ carboxylate groups of Na-EMAA with Ny6 appeared to be more efficient in promoting the Ny6/LDPE compatibility than Zn^{2+} carboxylate groups. This might be due to the fact that monovalent Na^+ ionomers are more prone to form strong ion-dipole interactions with amide groups of Ny6 than divalent Zn^{2+} counterparts, as a result of more stable ionic multiplets and more sterically hindred metal carboxylate ion pairs in ionomers containing divalent metal cations rather than monovalent ones.[9]

SEM micrographs of the fractured and etched surfaces of Ny6/Na-EMAA blends are shown in Figure 5. The d_n of the dispersed phase particles in these blends was approximately 1-2 μm, much smaller than the Ny6/LDPE/Na-EMAA blends. The distribution of sizes were more narrow in the two component blend vs. the three component blend.

As mentioned previously, a chemical reaction can occur between the primary amine groups and the carboxylic acid. The existence of this reaction was confirmed by the Molau test, which is carried out by adding the blends to 85% formic acid.[18,19] Figure 6 displays the appearance of the two bottles in which the Molau test were carried out for 80/20 Ny6/LDPE with and without 5 phr Na-EMAA5. The uncompatibilized blend gave, after strring with formic acid and several hours of settling, a clean separation of a transparent solution of Ny6 from the upper layer of LDPE particles. Addition of of Na-EMAA yields a third phase, which occurs as a white colloidal suspension in the liquid phase.[18-20]

SEM of the fractured surfaces of the Na-EMAA/LDPE binary blends at various blend ratios are shown in Figure 7. One phase materials are observed for the 20/80, 40/60, and 80/20 blends ratio (Figure 7a, b, e), whereas two phases, through

highly adherent, are clearly visible for the other two ratios (Figure 7c, d). The compatibility of these blends could be attributed to the miscible between polyethylene segments of LDPE and ethylene back bone segments of Na-EMAA.

WAXS Analysis

WAXS patterns of melt-crystallized samples for neat Ny6, LDPE, and Na-EMAA are presented in Figure 8, the scans for Ny6/Na-EMAA are shown in Figure 9, LDPE/Na-EMAA blends is shown in Figure 10, and for 50/50 Ny6/LDPE blends with and without Na-EMAA are shown in Figure 11. Pure Ny6 gave pronounced 2θ peaks at 20.2° and 23.5° associated with α_1-form (002) and α_2-form (200) crystal structure, respectively. A characteristic peak at 21.4° for the γ-form crystal structure was not observed. For pure LDPE, the scan showed an amorphous halo and two crystalline peaks at 21.38°, and 23.72° associated with orthorhombic (110) and (200) respectively were observed. Pure Na-EMAA specimen showed the same peaks at slightly different angles. For blends, peak positions at similar angles were observed, indicating that the crystalline structure of the blend was not affected by the Na-EMAA content.

TGA Analysis

The Arrhenius equation can be used to fit the kinetic behavior of experimental degradation data for the polymer under analysis.

$$d\alpha/dt \quad = \quad f(\alpha)\ A\ exp(-Ea/RT) \tag{3}$$

where; T is the temperature at a specific weight loss (K) and α is the reacted fraction at the time t, $f(\alpha)$ is a function of α depending on the reaction mechanism. The fractional conversion, α, was calculated using equation 4,

$$\alpha \quad = \quad \frac{(W_i - W)}{(W_i - W_f)} \tag{4}$$

where W_i is the initial weight of sample, W_f is the final weight of sample, W is the weight at a particular conversion. The Arrhenius equation is employed to determine the kinetic parameters, and the Flynn and Wall method is one of the simplest to

estimate these values. This approach chooses an arbitrary extent at a given temperature obtained from run at different heating rate, which assumes that $\alpha = 0.1$.

Figure 12 shows the TGA thermograms of pure Ny6, LDPE, Na-EMAA, and the 50/50 Ny6/LDPE with and without 5 phr of Na-EMAA. Pure LDPE showed an initial degradation temperature at around 280°C. Above this temperature free radicals are generated leading to sequential degradation and breakdown of the main chain due to the thermal decomposition of the covalent C-C bond at a higher temperature.[21] In the case of pure Ny6, a minor weight loss, associated with loss of bound water was initially observed, followed by major weight loss above 360°C, attributed to the breakdown of the main chain, evolving water, NH_3, CO_2, hydrocarbon fragments and CO.[22]

The thermal stability of the 50/50 Ny6/LDPE blend with and without Na-EMAA are somewhat intermediate between that of the homopolymers. Lamas suggested that for immiscible blends system, the onset of degradation was controlled by the behavior of the matrix component. Since LDPE is the matrix, the poor thermal stability of Ny6 and LDPE blends were attributed to poor thermal stability of LDPE.[5] The introduction of Na-EMAA into this blend induces intermolecular interactions between Ny6 and LDPE, and the blends with 5 phr of Na-EMAA has much greater thermal stability than the blend without Na-EMAA in the entire thermal decomposition range.

A measure of the thermal stability of Ny6/LDPE blends was calculated from the degradation temperature at 0.1 conversion. In the case of uncompatibilized blends, the thermal stability was much lower than that predicted by the rule of mixing in all the composition ranges. Although the degradation temperature and the activation energy of the blends increased with Ny6 content, these values were much lower when compared to the values obtained from the pure components. Thermal stability is very different when Na-EMAA was added into Ny6/LDPE blends. A positive deviation from simple additive mixing rule occurs, and a strong increase in activation energy is present confirming the previous observation that the addition of Na-EMAA led to a higher thermal stability of this blends. The thermal stability of compatibilized blends are slightly dependant on the Na-EMAA concentration. Ny6-

rich blends showed the higher degradation temperature, which is dominated by the high thermal stability of Ny6 matrix phase. Only 0.5 phr of Na-EMAA was enough to improve thermal stability of the 80/20 Ny6/LDPE blends, as the degradation temperature at 395.7°C was slightly higher than pure Ny6 (380°C). As described previously, the morphology obtained from SEM micrograph showed that 0.5 phr of Na-EMAA is sufficient to produce a maximum of the dispersed phase sizes.

The degradation temperature of LDPE/Na-EMAA blends increased with increasing amount of Na-EMAA, but the level of Na-EMAA did not affect the degradation temperature of the Ny6/Na-EMAA blends. However, the addition of Na-EMAA did increase the degradation temperature relative to pure Ny6 as shown in Figure 3. The effect of the metal counter ion of ionomers to the thermal stability of the blends are in agreement with the results from SEM analysis. The Na^+ carboxylate ionomers give higher thermal stability, demonstrated by the stronger increase of the degradation temperature and the activation energy over most of the blend composition range, this might be attributed to the higher interactions occurred between Na^+ carboxylate ionomers with amide groups of Ny6 than Zn^{2+} ones. This result could be due to the higher strength and stability of the ionic cross-links through ionic aggregation in the divalent Zn^{2+} ionomers compared with the monovalent Na^+ ionomers.[23]

DSC Analysis

Figure 16 and 17 show DSC cooling and heating scans for Ny6/Na-EMAA and LDPE/Na-EMAA binary blends. Pure Ny6 gave a crystallization temperature, T_c, of 187°C and two distinct melting points, T_m at 215°C and 222°C. Normally the melting endotherm of pure Ny6 appears as a main peaks at 221°C and a shoulder at 213°C, corresponding to α- and γ-form crystals, respectively.[7] The pure LDPE showed T_c at 88.8°C and T_m of 105.2°C and the pure Na-EMAA ionomer gave T_c of 62.3°C and a T_m of 94.7°C. The crystallization exotherm of Ny6 shifted to lower temperature as compared to pure Ny6 in the Na-EMAA/Ny6 blends, indicating that Na-EMAA inhibits Ny6 crystallization. The most likely explanation is the reduced mobility of the Ny6 due to molecular level interactions of the Ny6 with the ionomer. The T_c of the Na-EMAA increased with increasing Ny6 content, suggesting that Ny6 was

nucleating ethylene crystallization and enhancing the crystallization rate. Without nucleation, it is likely that ethylene crystallization would have slowed due to the reduced mobility caused by the interaction of acid segments with the Ny6.

The shape of the Ny6 melting endotherm varies significantly as compared to pure Ny6 for all compositions, especially in the case of 60/40 Ny6/Na-EMAA, which shows a broad peak, and in the 20/80 Ny6/Na-EMAA blend, which shows only one peak. The heat of fusion (ΔH_m), as well as the degree of crystallinity (χ_c) of Ny6 component are reduced when Na-EMAA is present (see Table 4), confirming that the strong interaction between Ny6 and Na-EMAA affects the crystallization of the former. For the LDPE/Na-EMAA blends, ΔH_m and χ_c of LDPE phase drop dramatically with an increase in Na-EMAA content as shown in Figure 5 due to the incorporation of methacrylic acid units into the ethylene chain increases the number of crystallizable ethylene segments. The curves are consistent with cocrystallization of the ethylene segments from the two materials. Surprisingly, the positions of the peaks in cooling behavior are not affected by the blend composition except in the high content ionomer material as shown in Figure 17.

As can be seen from the DSC thermograms of Ny6/LDPE blends, the characteristic behavior of immiscible system is exhibited, i.e. the cooling and melting thermograms of both components are completely independent of one another. The T_c of Ny6 in the ternary blend showed a slightly decrease with Na-EMAA content indicating again that the ionomer slows down the crystallization of Ny6. T_m of Ny6 and LDPE components decrease with increasing amount of Na-EMAA as shown in Table 6 consistent with the behavior found for the binary blends. When the Zn^{2+} ionomers was used as a compatibilizer instead of Na^+ ionomers, the crystallization behavior of the resulting blends were changed, and the T_c of both Ny6 and LDPE phases were reduced by a factor of 5°C as compared to Na^+ ionomers. For the Ny6, this indicates better the T_m of Ny6 and LDPE were not affected by the type of metal cation.

CONCLUSIONS

The ethylene-methacrylic acid copolymer partially neutralized with sodium (Na-EMAA) had been shown by a morphological and thermal investigation to behave as

an effective compatibilizer for Ny6/LDPE blends. Addition of small amounts of Na-EMAA reduce the dispersed phase size by approximately a factor 5, and as little as 0.5 phr of Na-EMAA was sufficient to produce a maximum reduction of dispersed phase size. The ionomers thermally stabilized both Ny6 and LDPE; the 80/20 Ny6/LDPE compatibilized with 0.5 phr of Na-EMAA gave the highest decomposition temperature, ca. 16°C higher than pure Ny6. The presence of Na-EMAA decreased the crystallization temperature of Ny6, indicating that Na-EMAA retarded nylon crystallization. Melting point depression phenomenon was found in both Ny6 and LDPE phases in the ternary blend, although the reasons for the depression was different. In the former case, the reason was attributed to the strong interaction between Ny6 and the ionomers which reduced both the fractional crystallinity and crystallite perfection, in the latter case the reason was attributed to short ethylene segment incorporation from the ionomers into polyethylene crystals. Although not from the same base resin nor the same neutralization level, the Na^+ carboxylate ionomers were a more effective compatibilizer than the Zn^{2+} ones due to the lower dispersed phase size and higher thermal stability of the resulting blends.

ACKNOWLEDGEMENTS

REFERENCES

1. Fairley, G., and Prud'homme, R.E., *Polym. Eng. Sci.*, 27(2), 1495-1503 (1987).
2. Armat, R., and Moet, A., *Polymer*, 34(5), 977-985 (1993).
3. Kudva, R.A., Keskkula, H., and Paul, D.R., *Polymer*, 40, 6003-6021 (1999).
4. Halldén, Åsa, Deriss, M.J., and Wesslén, B., *Polymer*, 42, 8743-8751 (2001).
5. Lamas, L., Mandes, G.A., Müller, A.J., and Pracella, M., *Eur. Polym. J.*, 34(12), 1865-1870 (1998).
6. Minkova, L., Yordanov, Hr., and Filippi, S., *Polymer*, 43(23), 6195-6204 (2000).
7. Psarski, M., Pracella, M., and Galeski, A., *Polymer*, 41(13), 4923-4932 (2000).
8. Valenza, A., Visco, A.M., and Acierno, D., *Polymer Testing*, 21, 101-109 (2002).

9. Degée, Ph., Vankan, R., Teyssié, Ph., and Jérôme, R., *Polymer*, 38(15), 3861-3867 (1997).

10. Valenza, A., Geuskens, G., and Spadaro, G., *Eur. Polym. J.*, 33(6), 957-962 (1997).

11. Leewajanakul, P., Pattanaolarn, R., Ellis, J.W., Nithitanakul, M., Grady, B.P., *J. Appl. Polym. Sci.*, 89, 620-629 (2003).

12. Macknight, W.J., and Lenz, R.W., *Polym. Eng. Sci.*, 25(18), 1124-1133 (1985).

13. Sheng, J., Ma, H., Yuan, X.B., Yuan, X.Y., Shen, N.X., and Bian, D.C., *J. Appl. Polym. Sci.*, 76, 488-494 (2000).

14. Willis, J.M., and Favis, B.D., *Polym. Eng. Sci.*, 28, 1416-1426 (1988).

15. Willis, J.M., Favis, B.D., and Lavallee, C., *J. Mater. Sci.*, 28, 1749-1757 (1993).

16. Yeh, J.T., Fan-Chiang, C.C., and Cho, M.F., *Polymer bulletin*, 35, 371-378 (1995).

17. Sánchez, A., Rosales, C., Laredo, E., Müller, J.A., and Pracella, M., *Macromol. Chem. Phys.*, 202, 2461-2478 (2001).

18. Han, D.C., and Chuang, H., *J. Appl. Polym. Sci.*, 30, 2431-2455 (1985).

19. Scaffaro, R., La Mantia, P.F., Canfora, L., Polacco, G., Filippi, S., Magagnini, P., *Polymer*, 44, 6951-6957 (2003).

20. Anttila, U., Hakala, K., Löfgren, B., Seppälä, J., *J. Polym. Sci. :Part A: Polym. Chem*, 37, 3099-3109 (1999).

21. Jana, R.N., Mukunda, P.G., and Nando, G.B., *Poly. Degrad. Stab.*, 80, 75-82 (2003).

22. Albano, C., and Freitas, D.E., *Poly. Degrad. Stab.*, 61, 289-295 (1998).

23. Ma, X., Sauer, J.A., and Hara, M. *Macromolecule*, 28, 3953-3962 (1995).
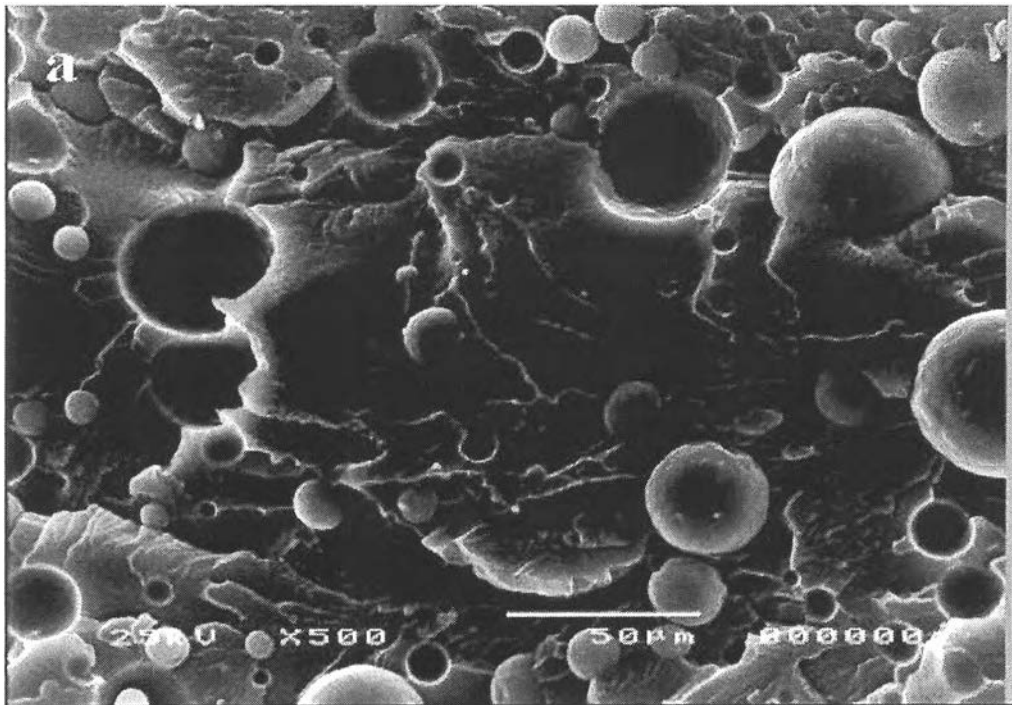
(a) 20/80 Ny6/LDPE
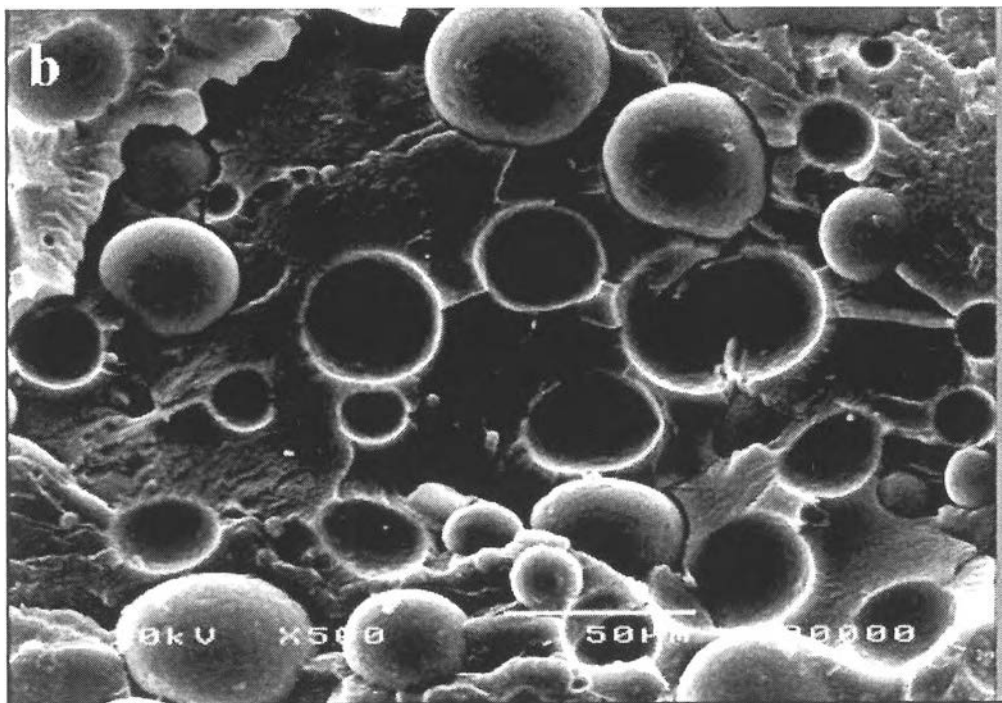
(b) 40/60 Ny6/LDPE
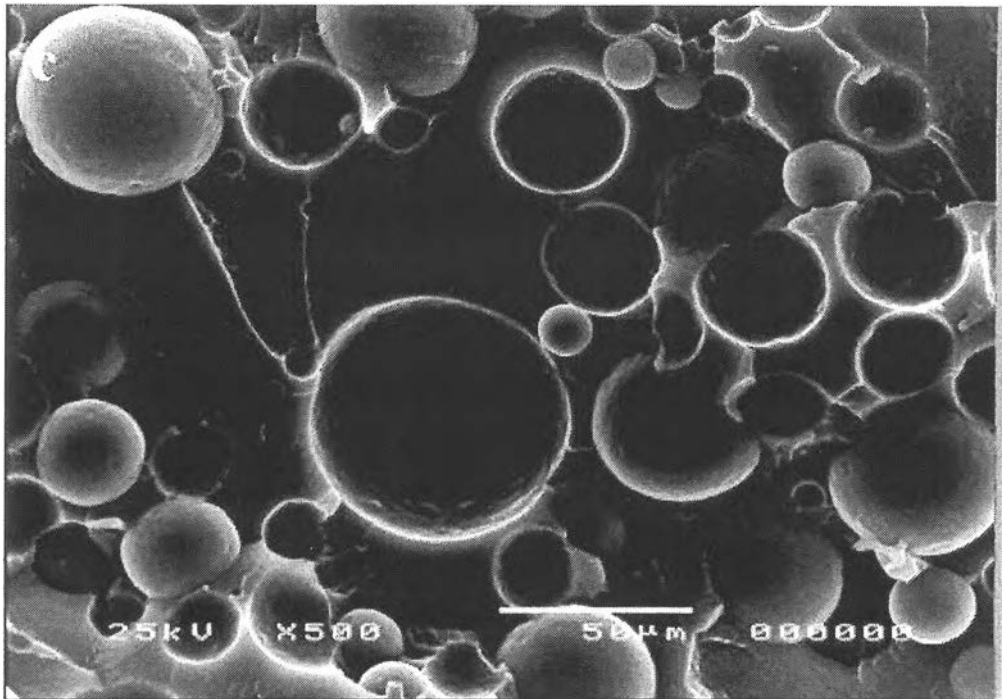
(c) 50/50 Ny6/LDPE
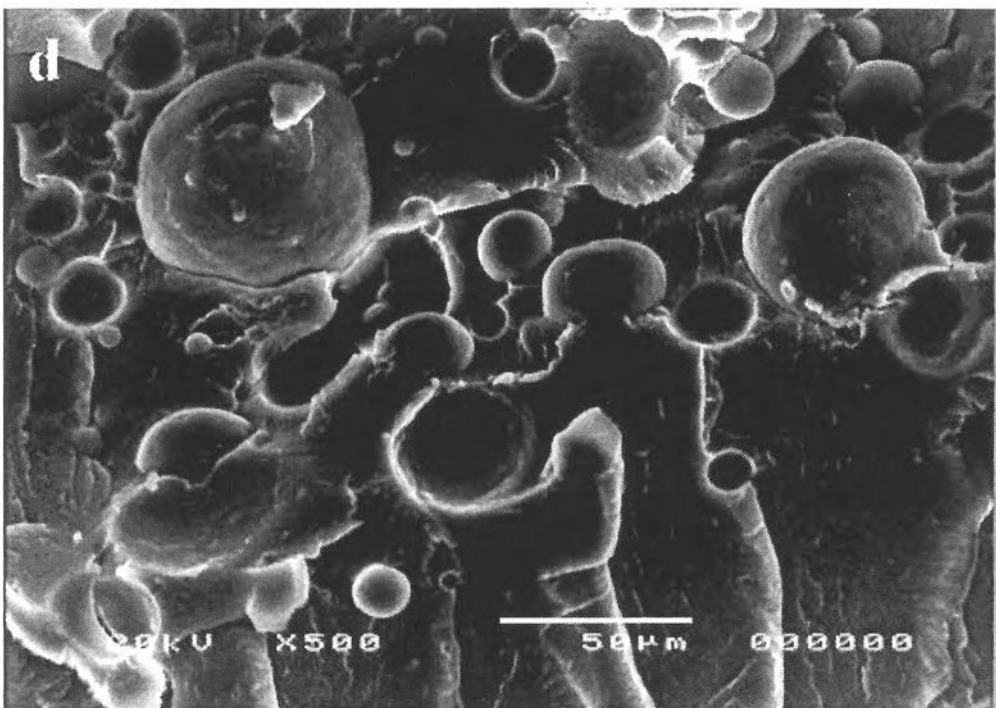
(d) 60/40 Ny6/LDPE
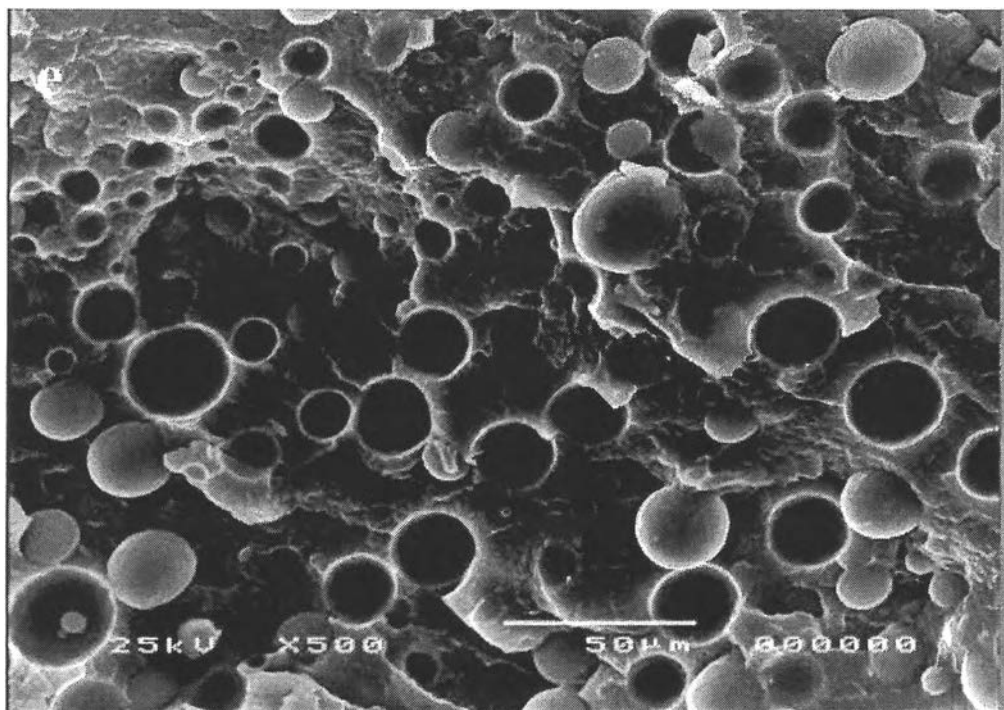
(e) 80/20 Ny6/LDPE

Figure 1 Scanning electron micrographs of fractured surfaces of uncompatibilized Ny6/LDPE blends.
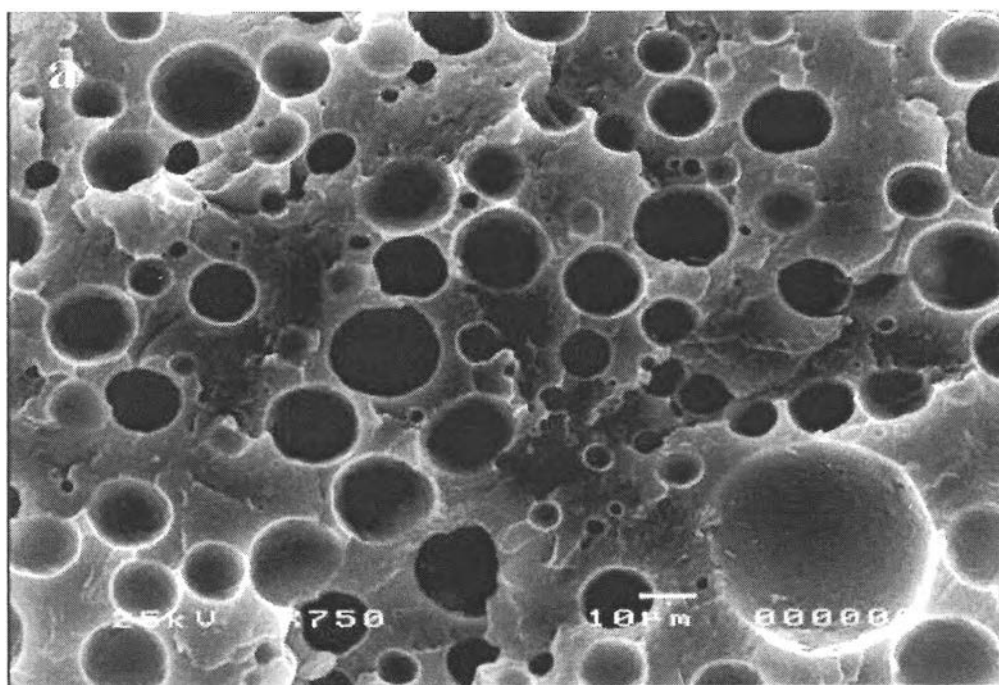
(a) Without Na-EMAA
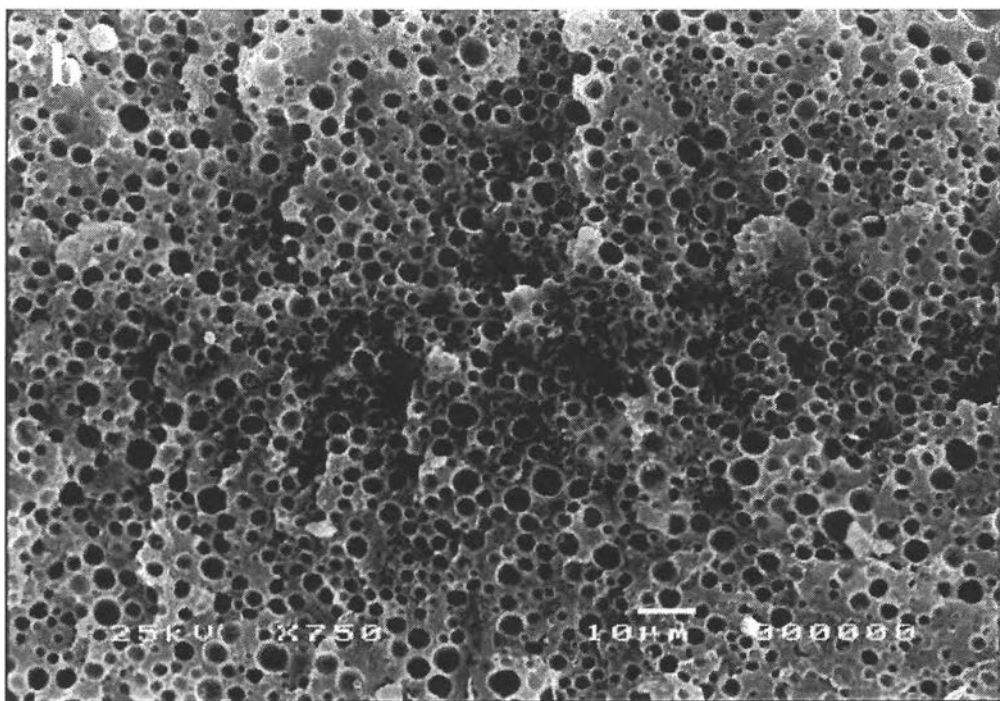
(b) With 0.5 phr of Na-EMAA
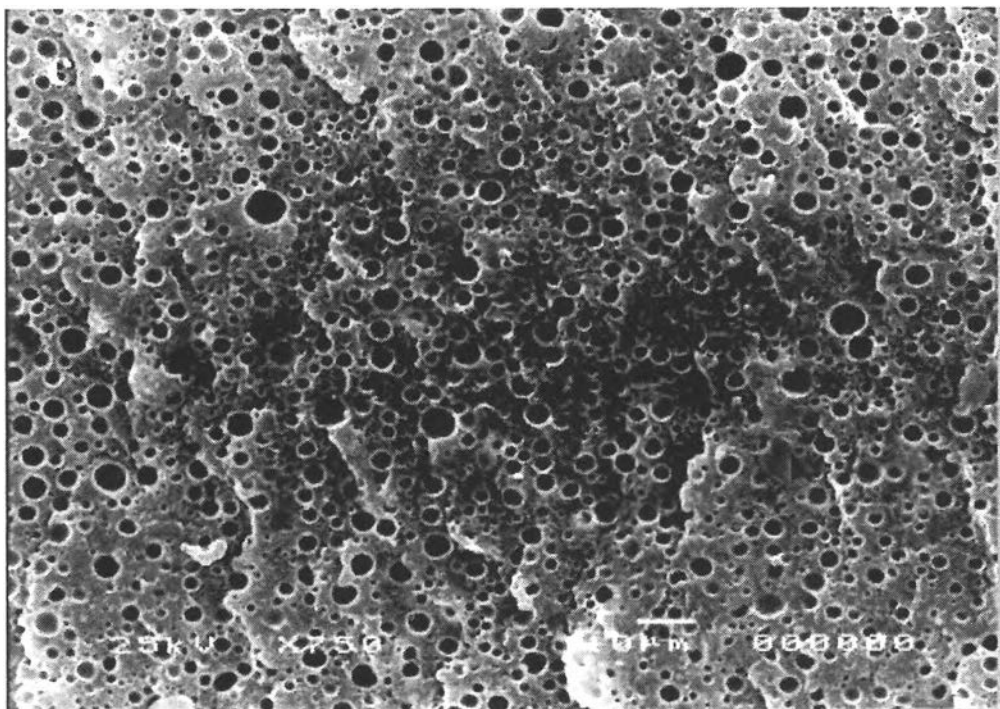
(c) With 1.5 phr of Na-EMAA
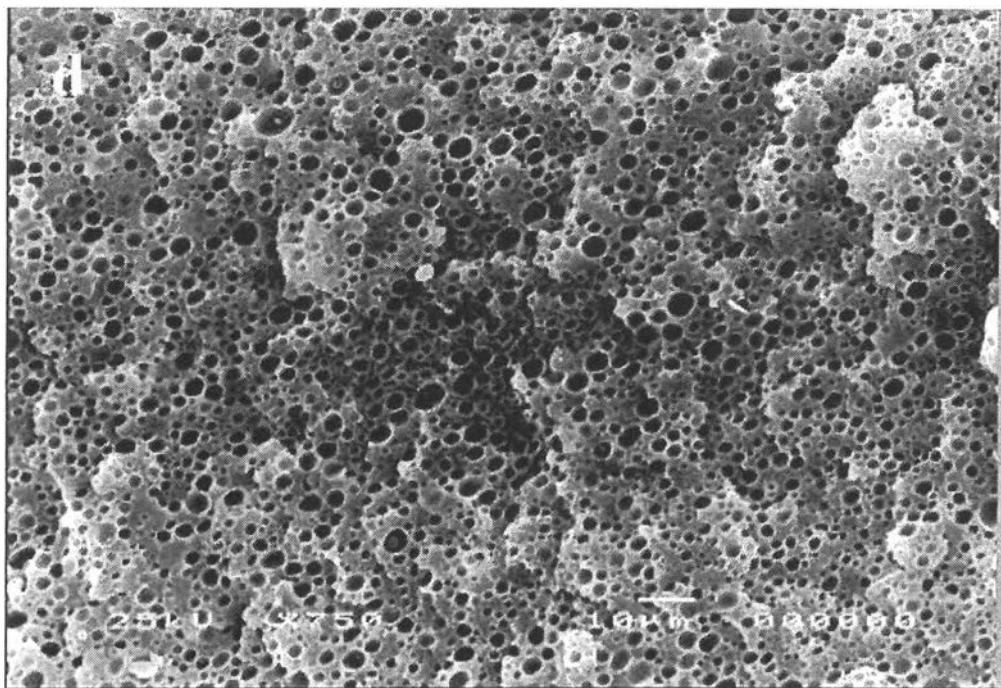
(d) With 5.0 phr of Na-EMAA

Figure 2 Scanning electron micrographs of fractured and etched surfaces of 80/20 Ny6/LDPE blends after immersion in hot decalin.
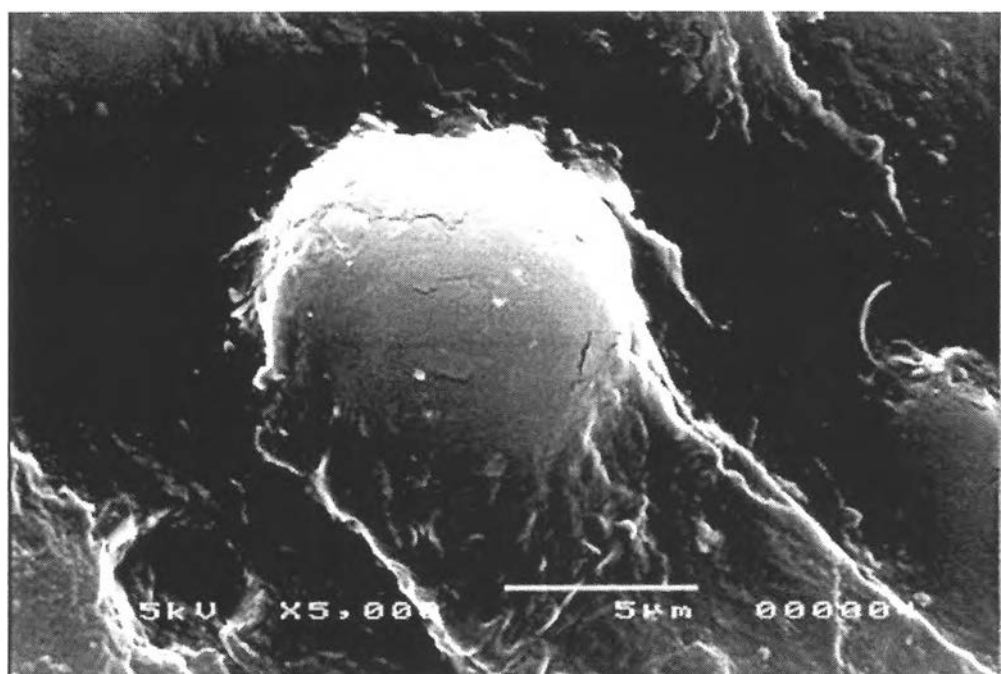
Figure 3 Scanning electron micrographs of fractured surfaces of 20/80, Ny6/LDPE blend compatibilized with Na-EMAA 0.5 phr.
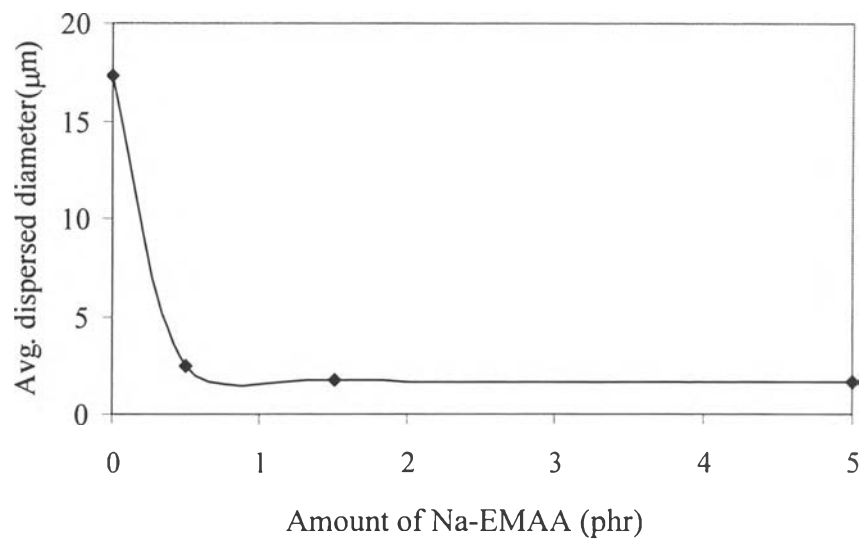
Figure 4 The dependence of the number average diameters measured as a function of the Na-EMAA content of 80/20 Ny6/LDPE blends.
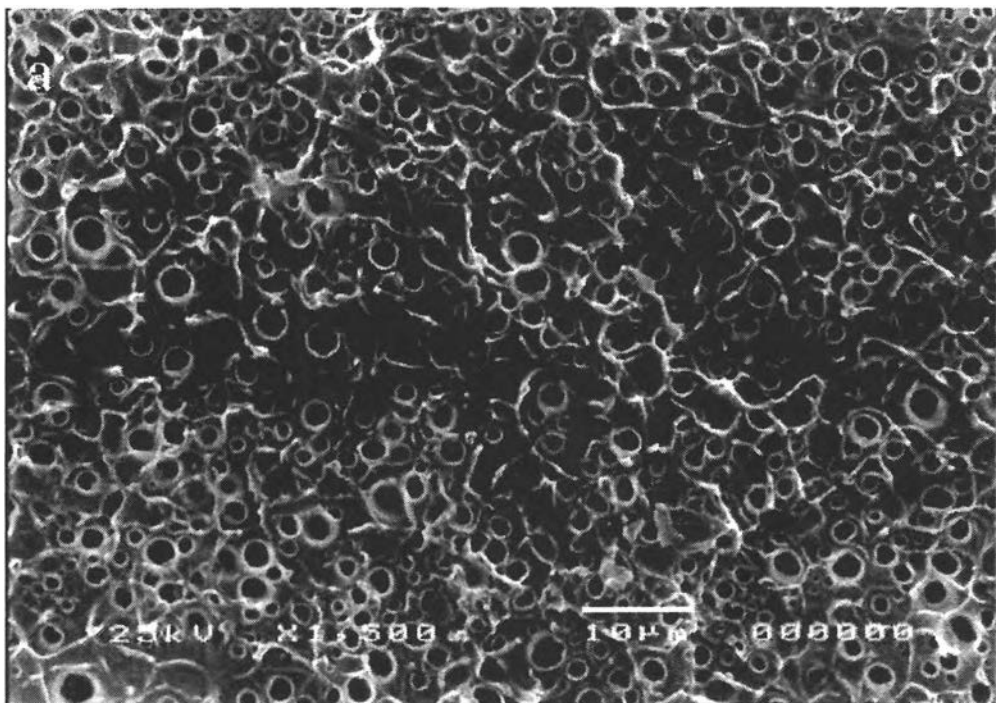
(a) 20/80 Ny6/Na-EMAA
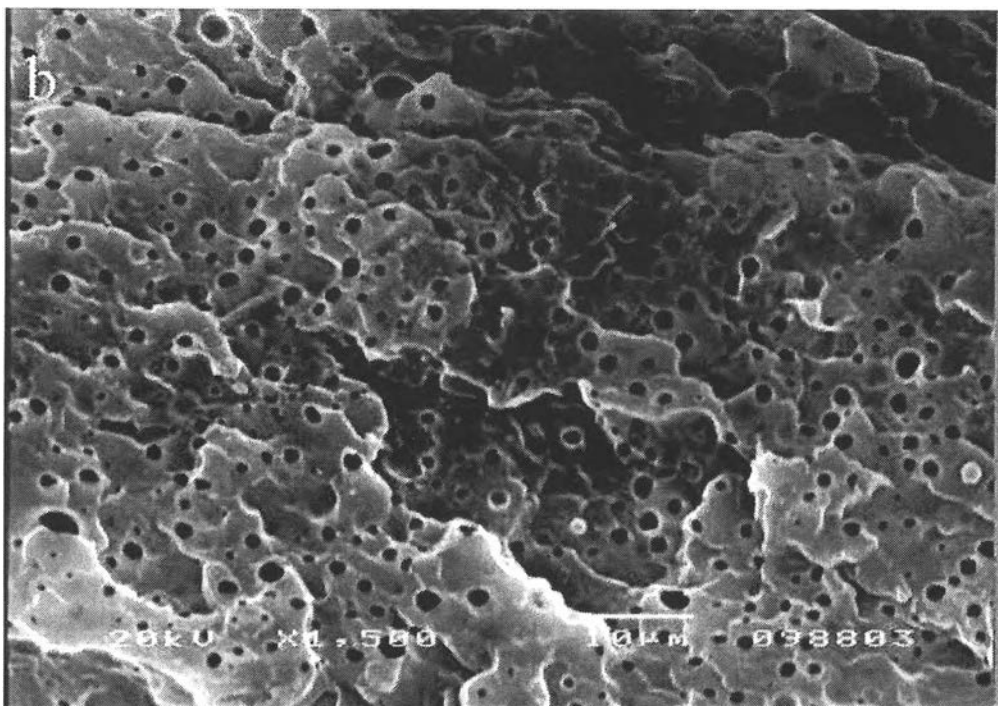
(b) 40/60 Ny6/Na-EMAA
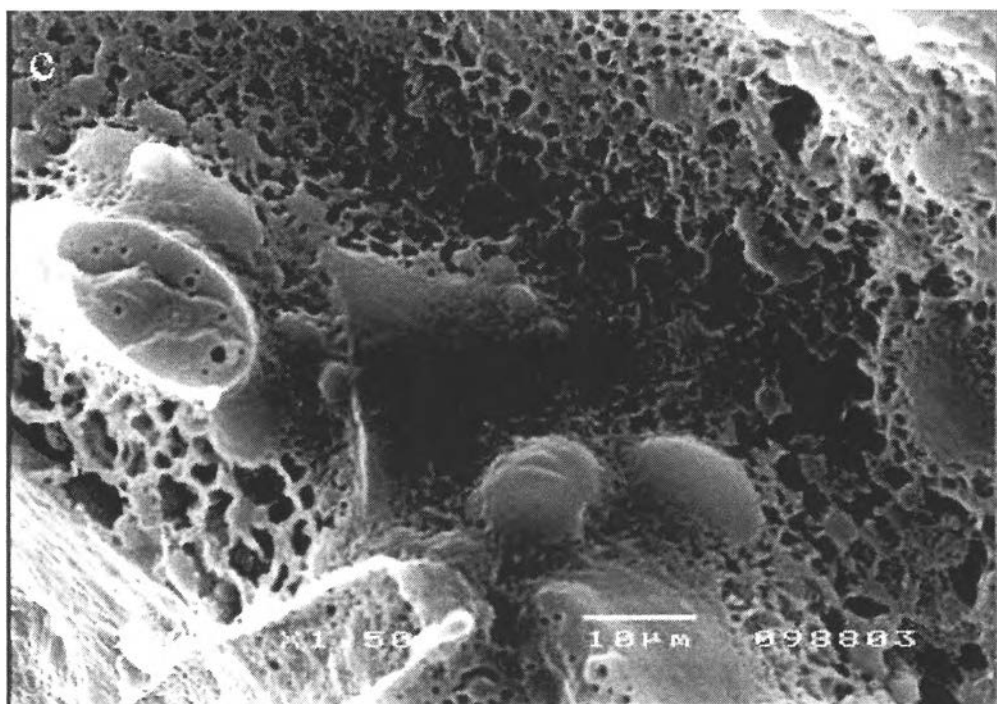
(c) 50/50 Ny6/Na-EMAA
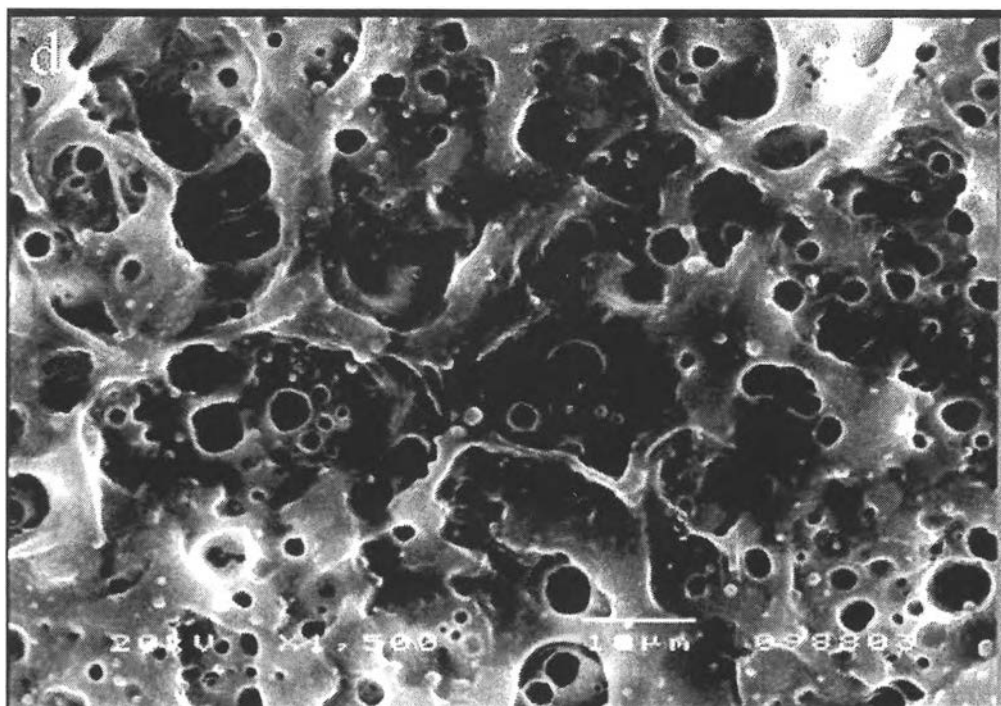
(d) 60/40 Ny6/Na-EMAA
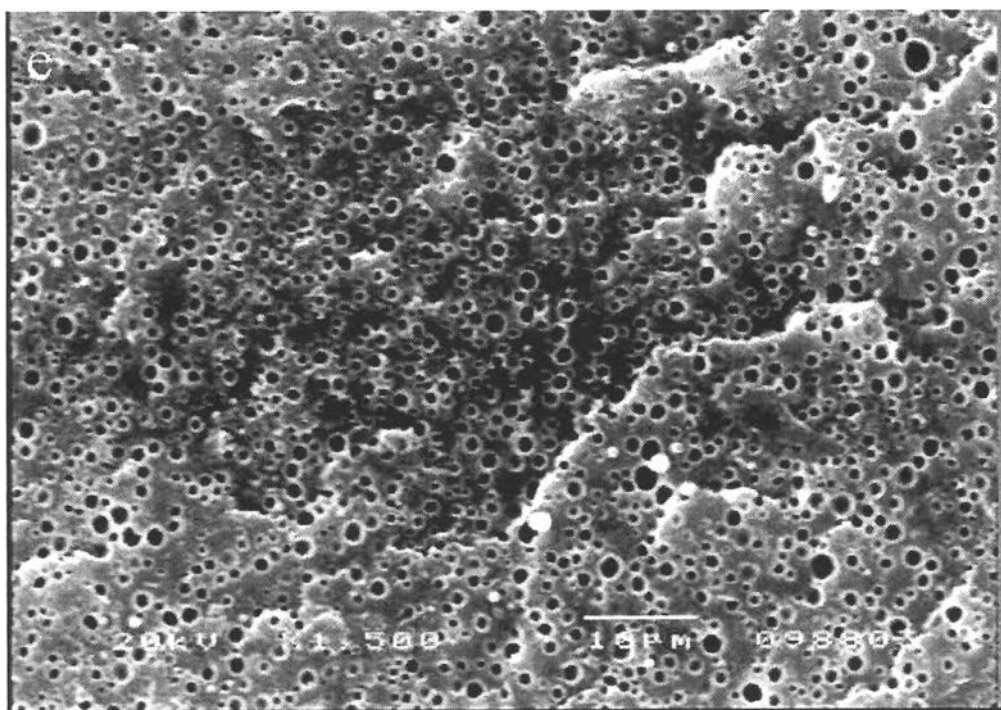
(e) 80/20 Ny6/Na-EMAA

Figure 5 Scanning electron micrographs of fractured surfaces of Ny6/Na-EMAA blends.
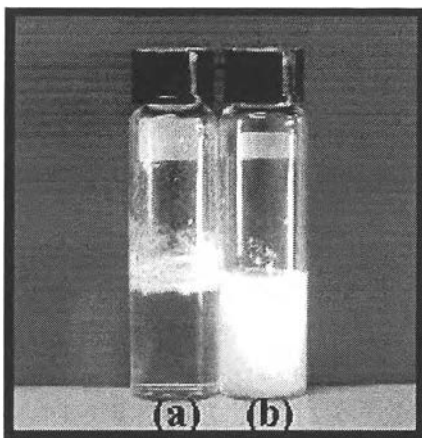
Figure 6 Molau test solutions consisting of 85% formic acid added to each of the following blends: (a) 80/20 Ny6/LDPE, (b) 80/20/5 Ny6/LDPE/Na-EMAA.
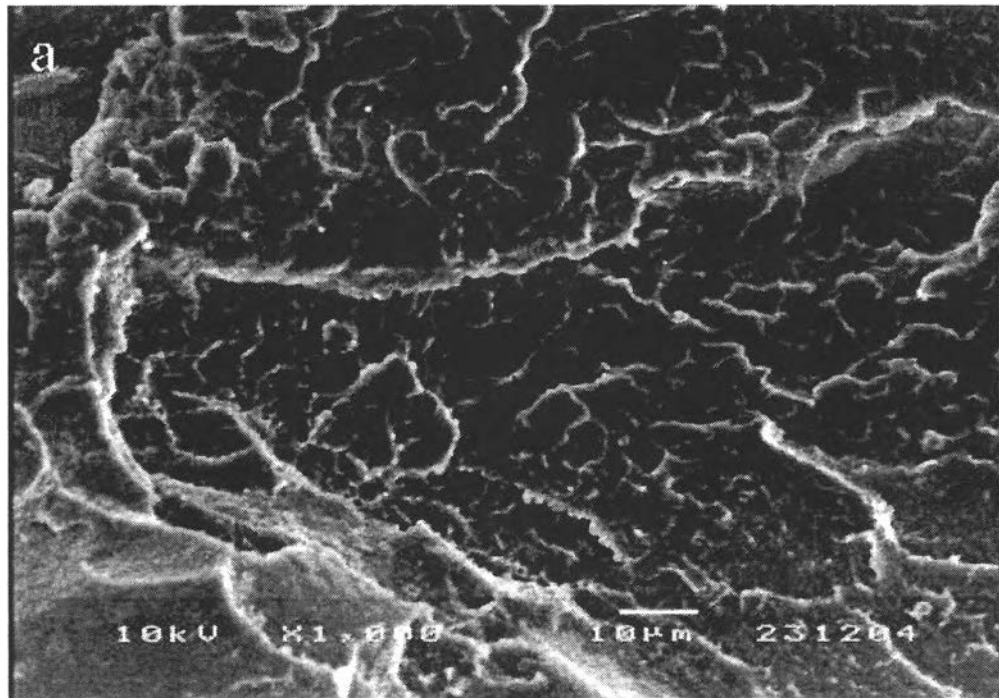
(a) 20/40 LDPE/Na-EMAA
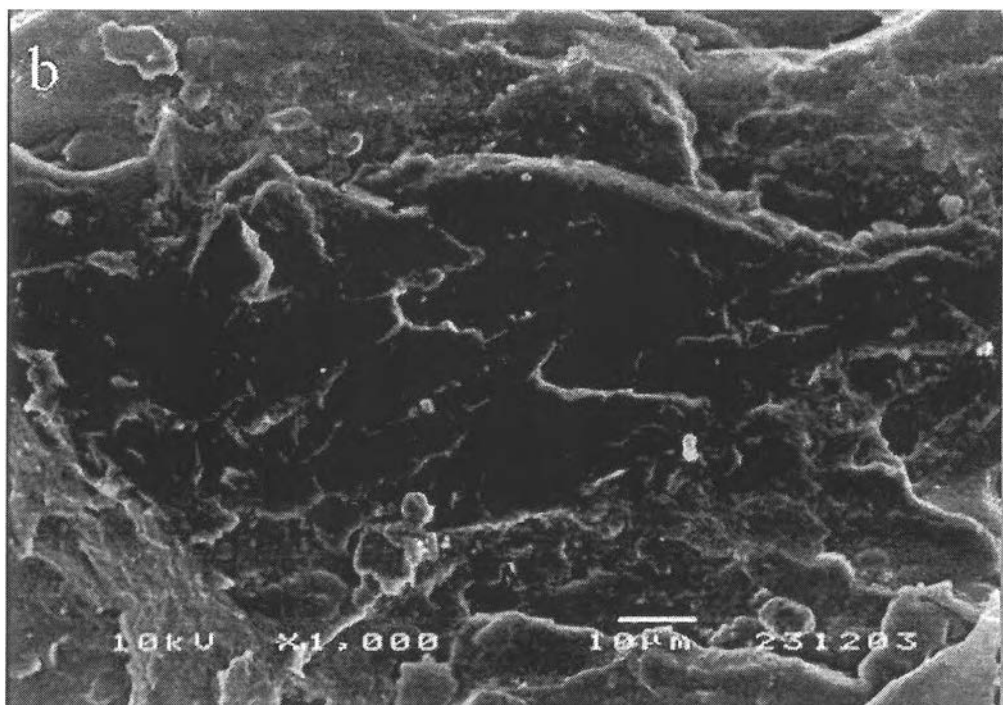
(b) 40/60 LDPE/Na-EMAA
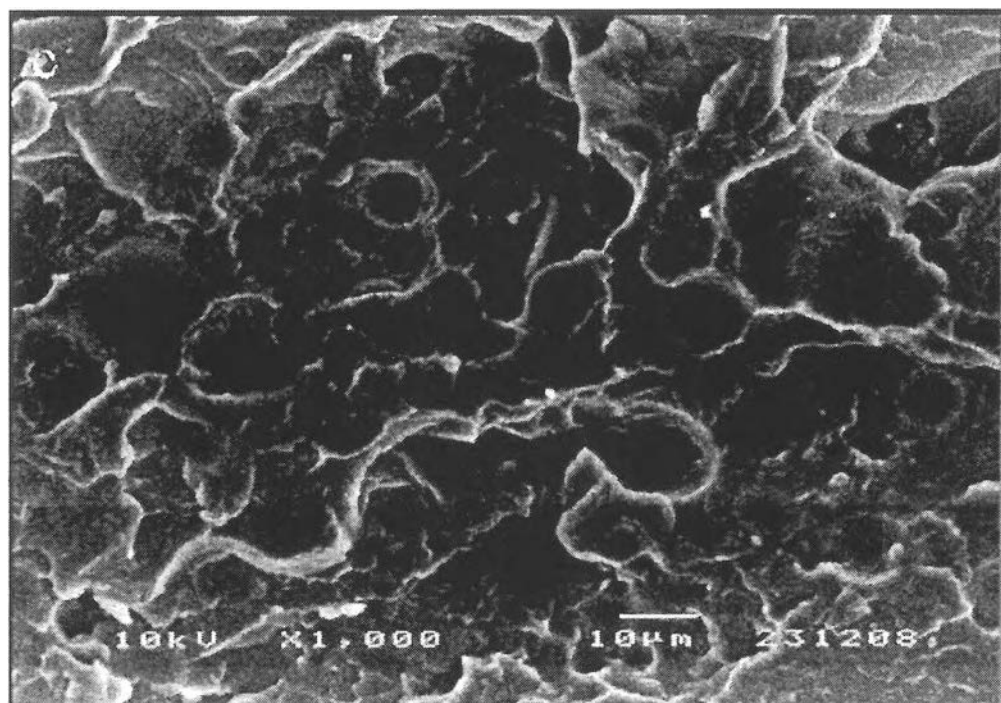
(c) 50/50 LDPE/Na-EMAA
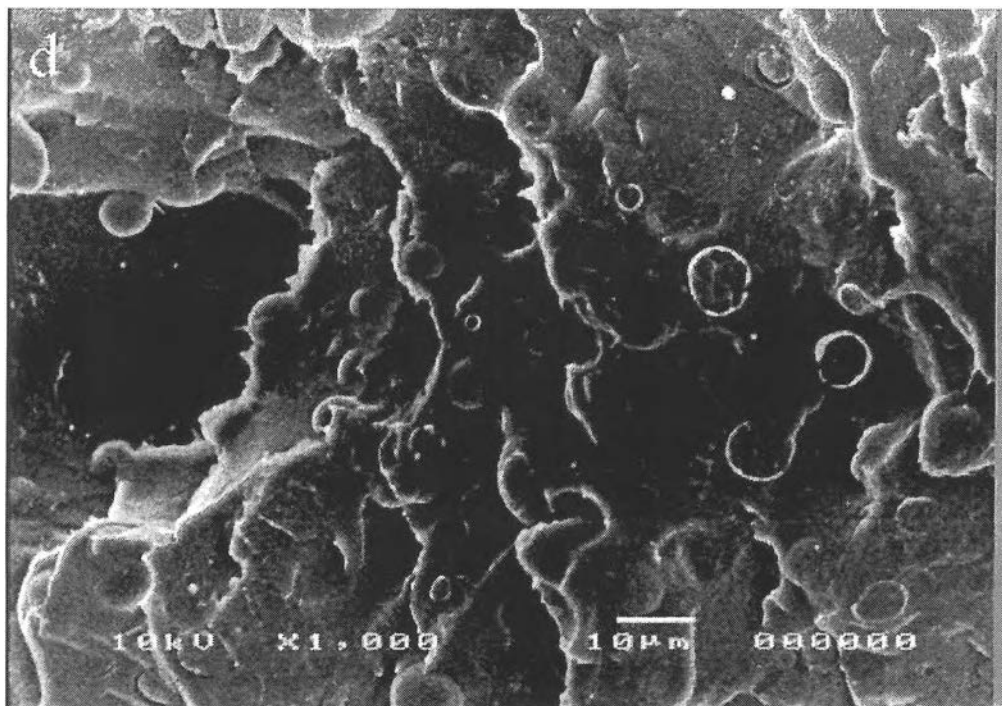
(d) 60/40 LDPE/Na-EMAA
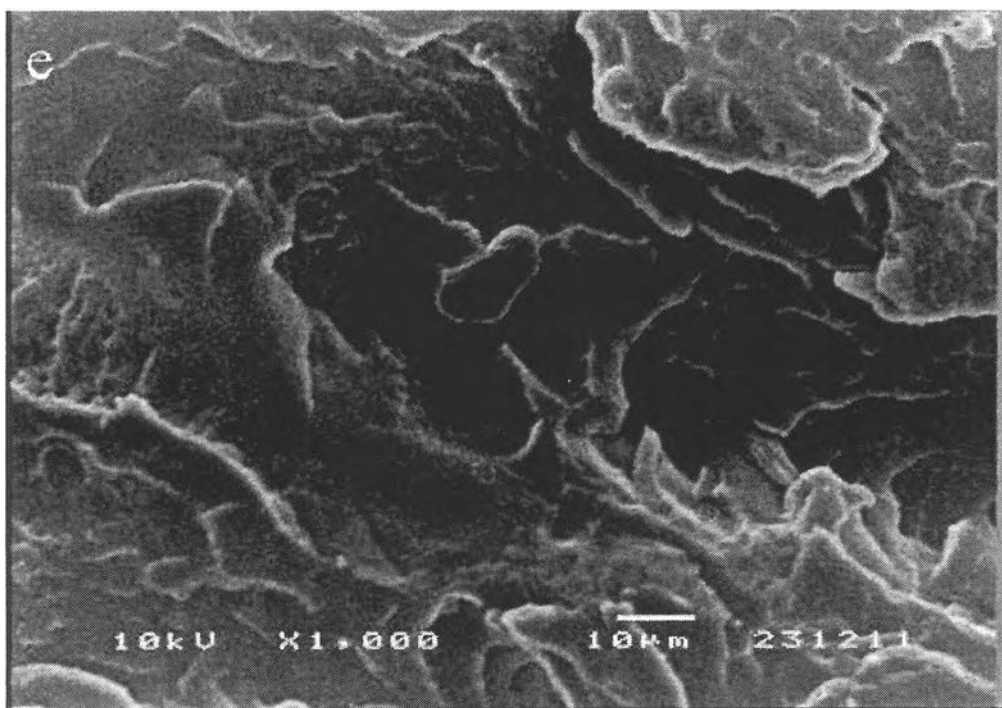
(e) 80/20 LDPE/Na-EMAA

Figure 7 Scanning electron micrographs of fractured surfaces of LDPE/Na-EMAA blends.
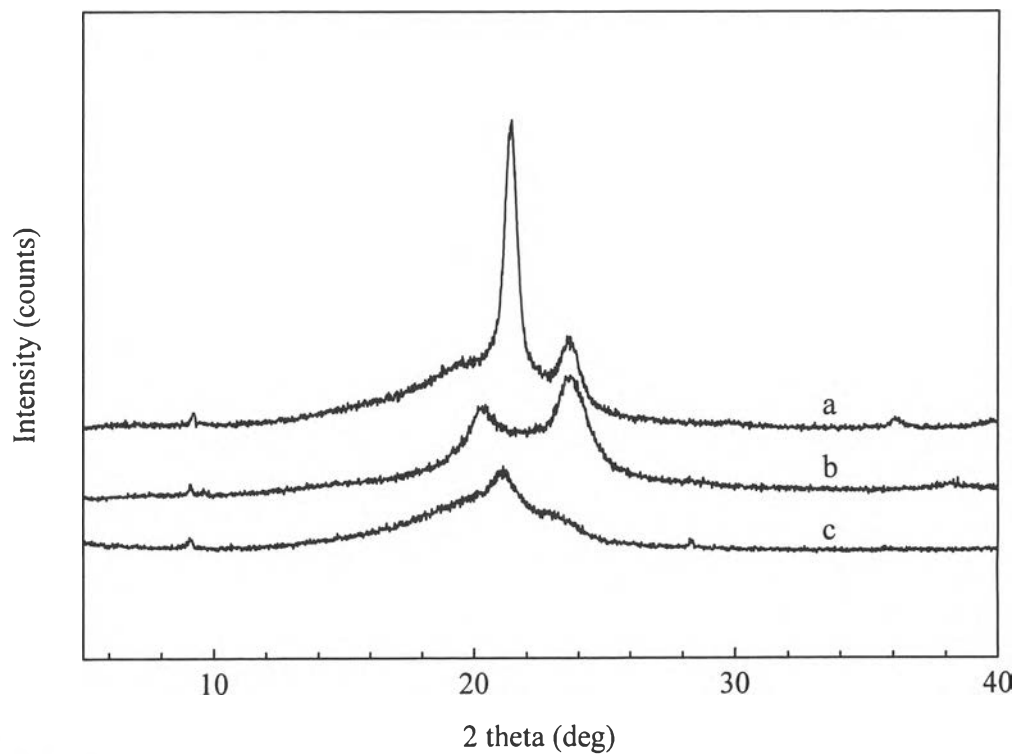
Figure 8 WAXS patterns of pure polymers: (a) LDPE, (b) Ny6, and (c) Na-EMAA.
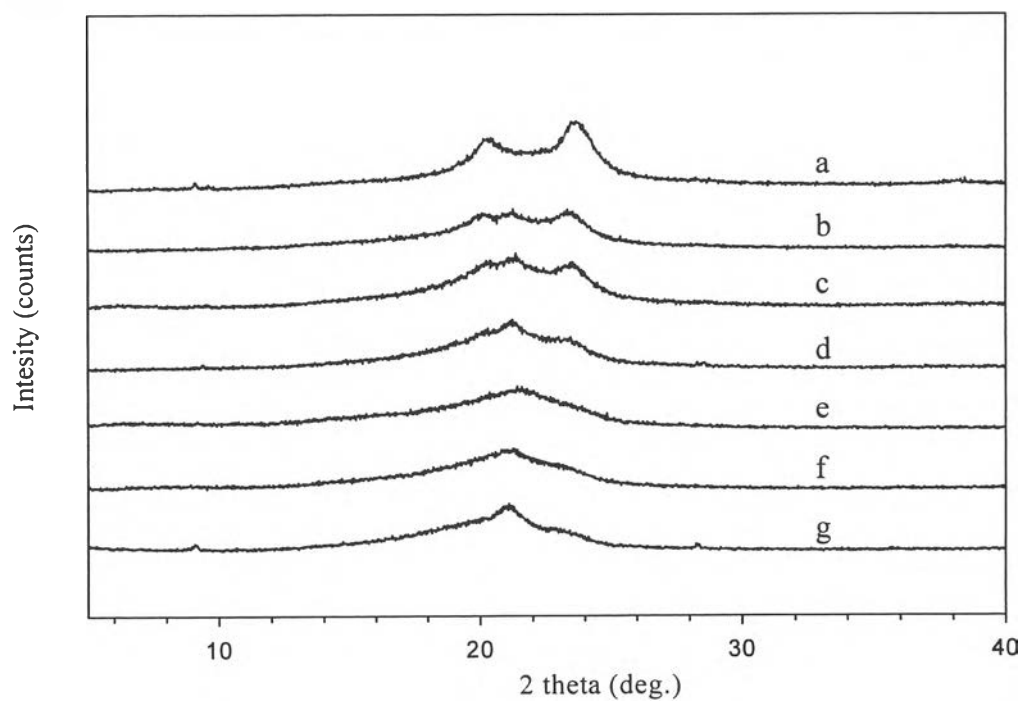
Figure 9 WAXS patterns of Ny6/Na-EMAA blends: (a) Ny6, (b) 80/20, (c) 60/40, (d) 50/50, (e) 40/60, (f) 20/80, and (g) Na-EMAA.
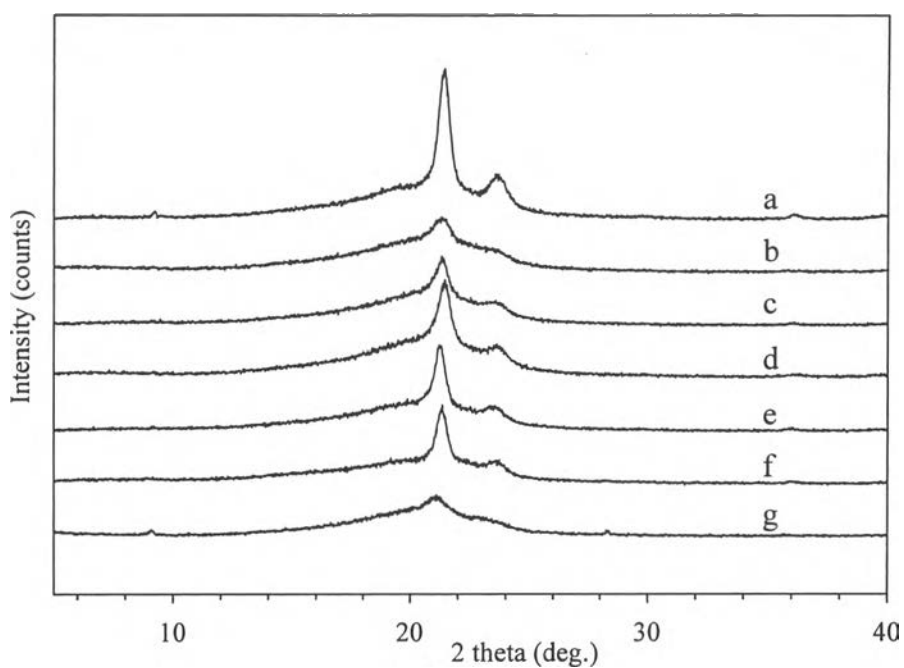
Figure 10 WAXS patterns of LDPE/Na-EMAA blends: (a) LDPE, (b) 20/80, (c) 40/60, (d) 50/50, (e) 60/40, (f) 80/20, and (g) Na-EMAA.
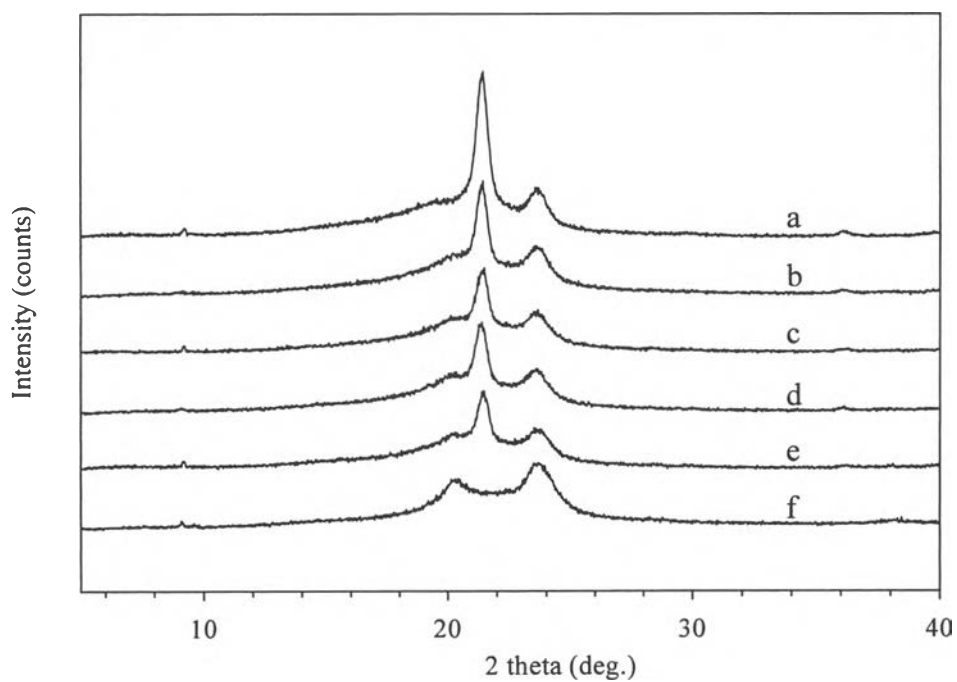
Figure 11 WAXS patterns of 50/50 Ny6/LDPE blends: (a) LDPE, (b) 5.0 phr, (c) 1.5 phr, (d) 0.5 phr , (e) 0 phr of Na-EMAA, (f) Ny6.
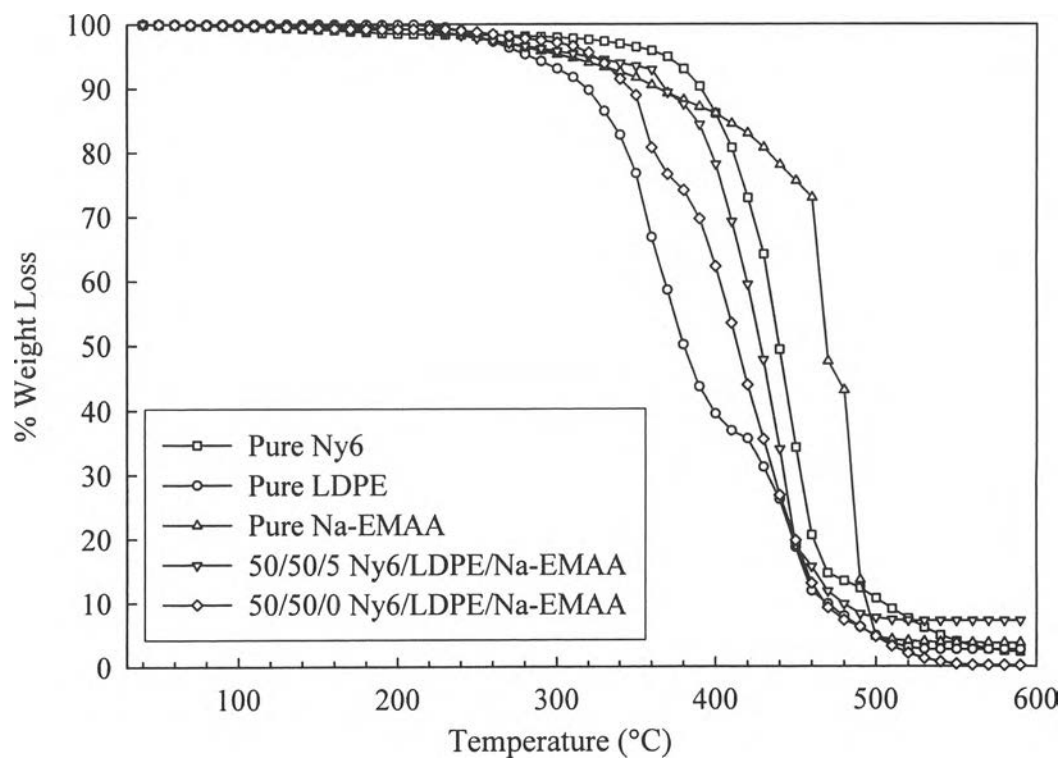
Figure 12 TGA curves at 10°C/min of neat polymers and 50/50 Ny6/LDPE and Ny6/LDPE with 5.0 phr Na-EMAA.
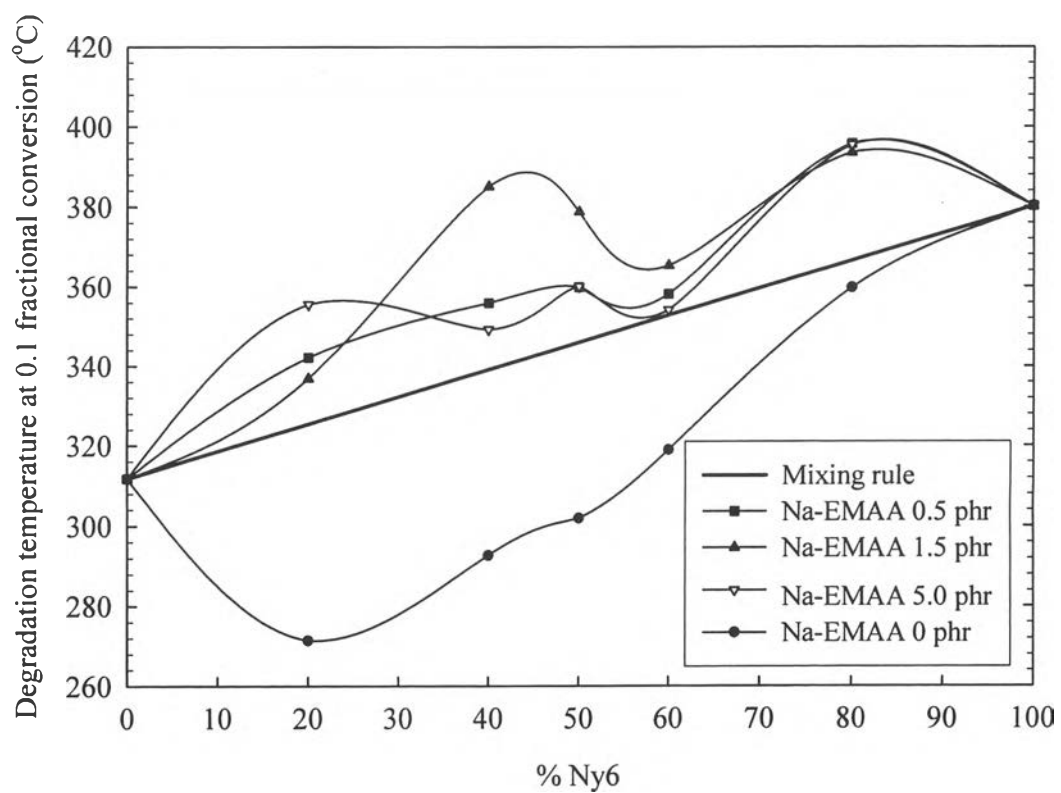
Figure 13 Degradation temperature at 0.1 fractional conversion of Ny6/LDPE blends.
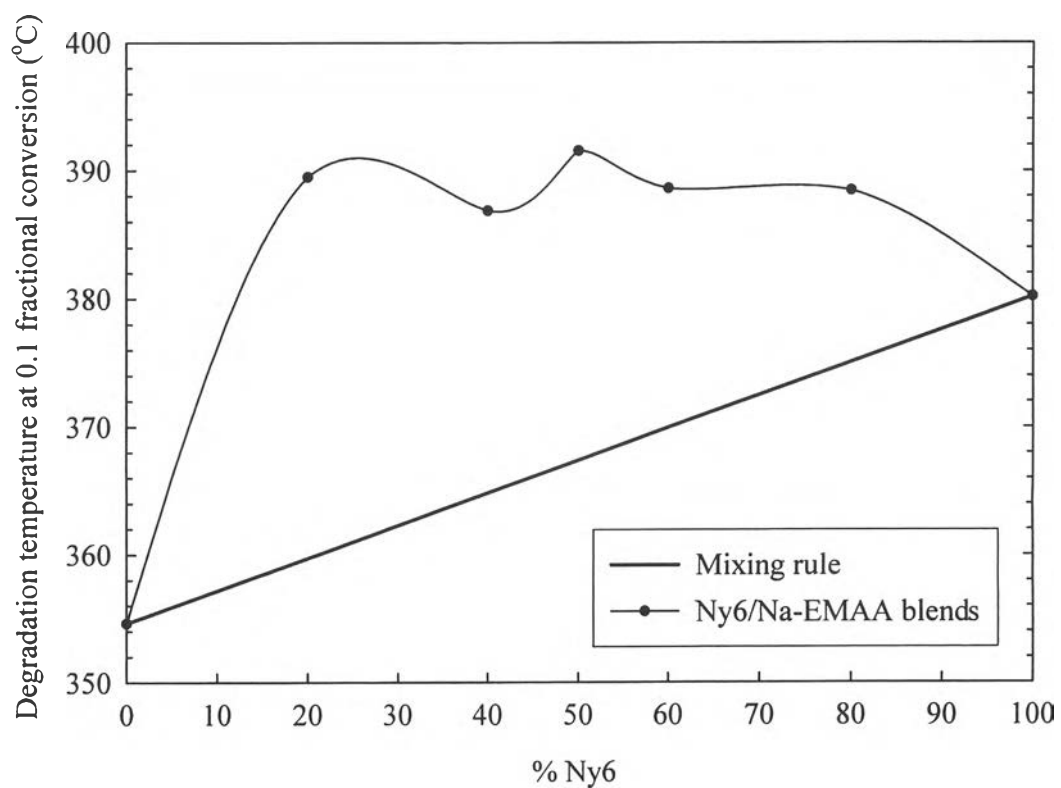
Figure 14 Degradation temperature at 0.1 fractional conversion of Ny6/Na-EMAA blends.
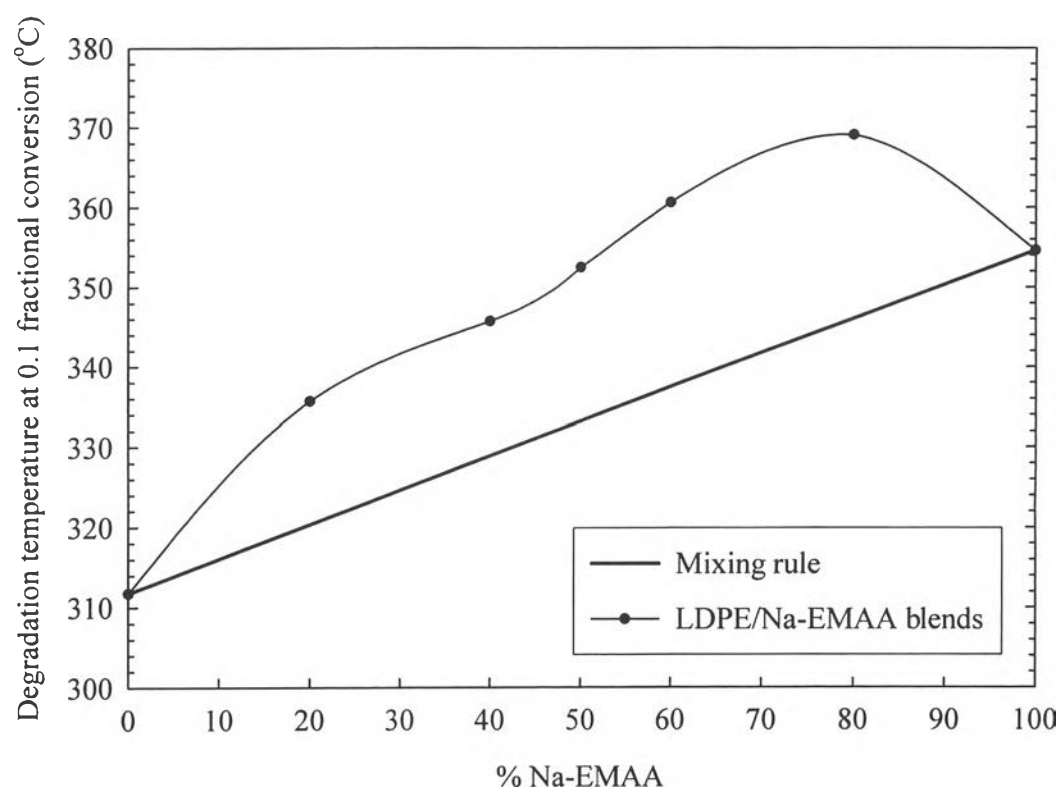
Figure 15 Degradation temperature at 0.1 fractional conversion of LDPE/Na-EMAA blends.
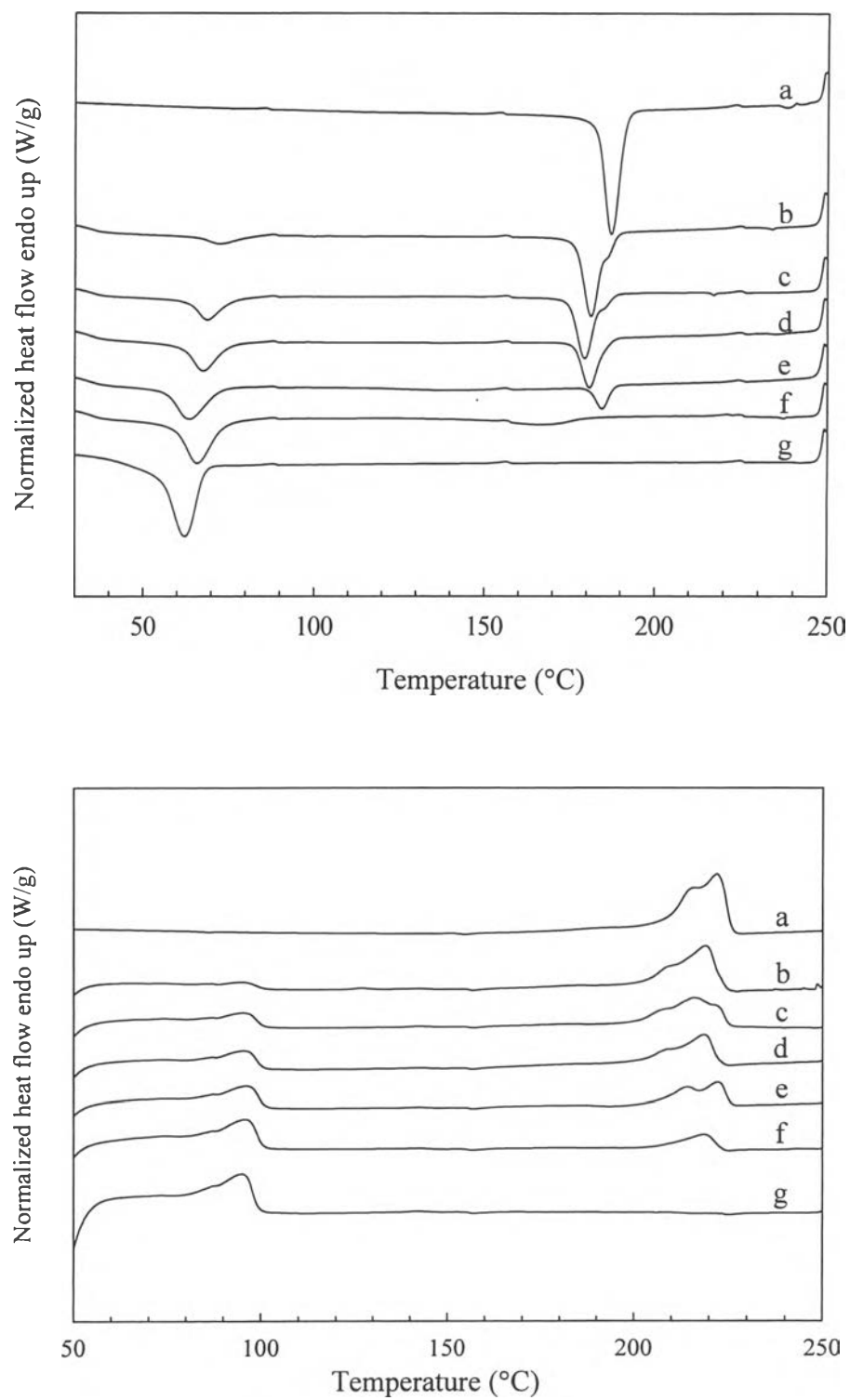
Figure 16 DSC thermograms of Ny6/Na-EMAA blends: (a) Ny6, (b) 80/20, (c) 60/40, (d) 50/50, (e) 40/60, (f) 20/80, (g) Na-EMAA.
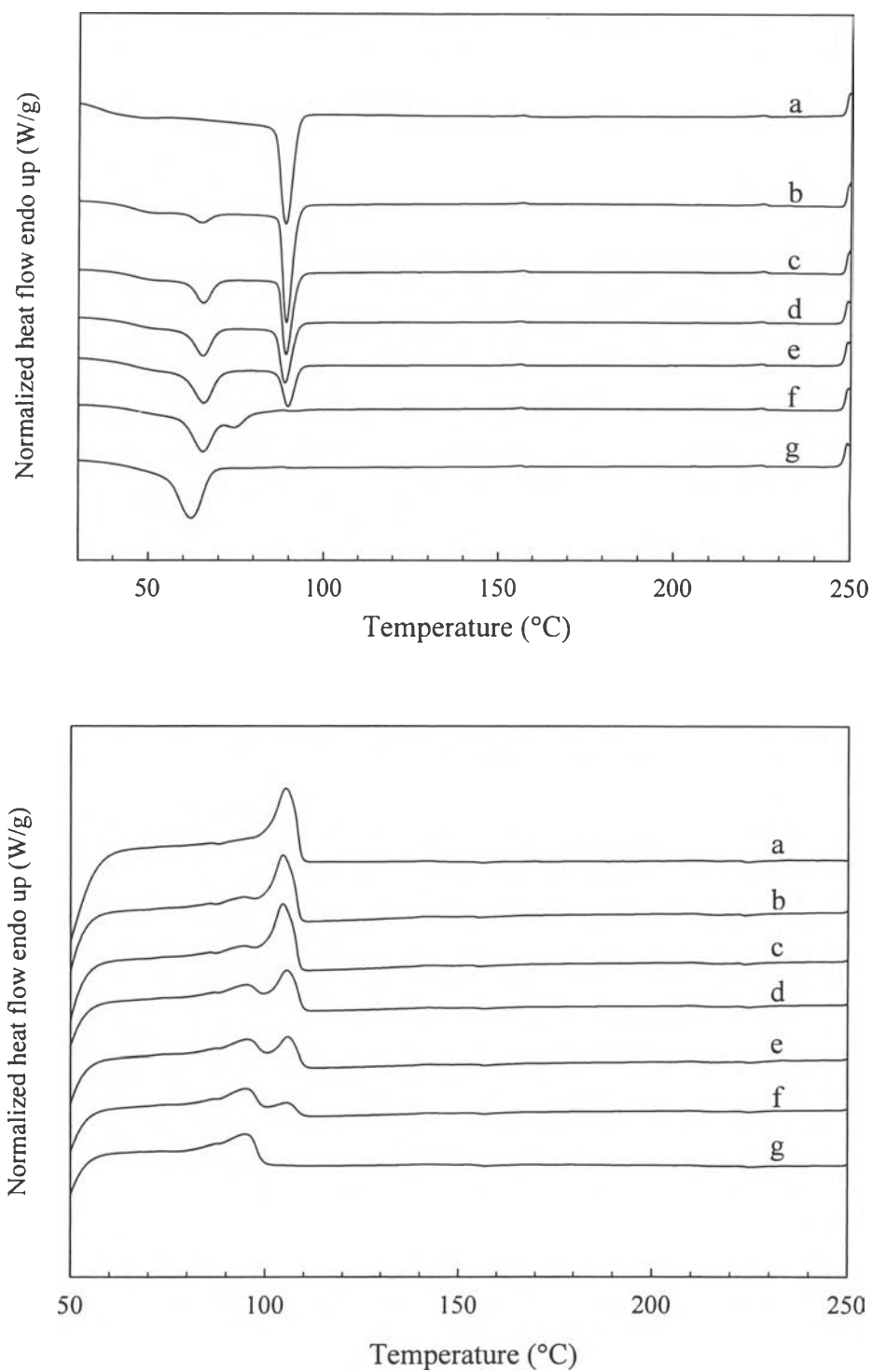
Figure 17 DSC thermograms of LDPE/Na-EMAA blends: (a) LDPE, (b) 80/20, (c) 60/40, (d) 50/50, (e) 40/60, (f) 20/80, (g) Na-EMAA.
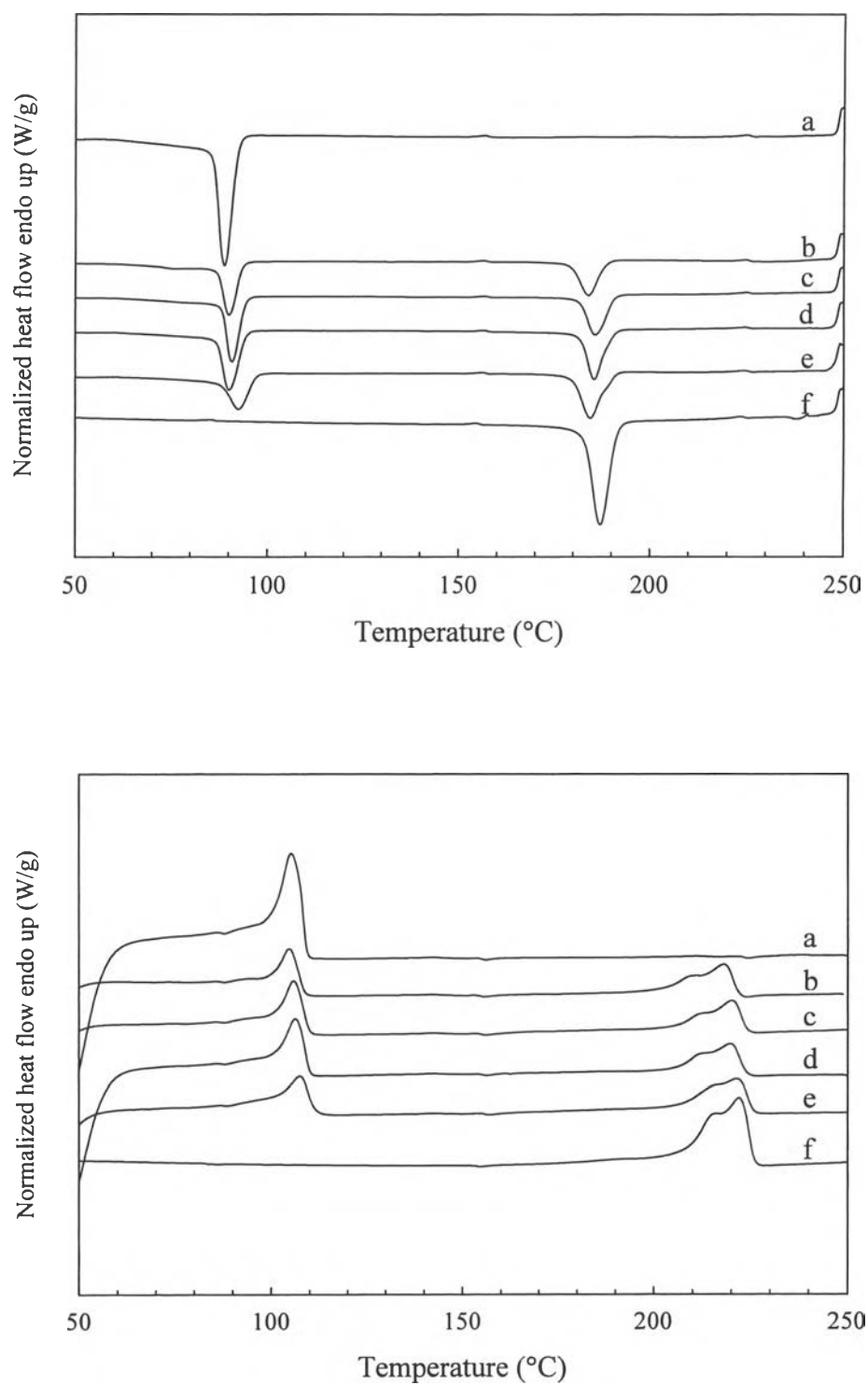
Figure 18 DSC thermograms of 50/50 Ny6/LDPE blends: (a) LDPE, (b) 5.0 phr, (c) 1.5 phr, (d) 0.5 phr, (e) 0 phr of Na-EMAA, (f) Ny6.

Table 1 Number average diameter of dispersed phase size of blends.

Blend type	Number average diameter (μm)									
Ratio (%wt)	20/80		40/60		50/50		60/40		80/20	
Metal ion type	Na^+	Zn^{2+}	Na^+	Zn^{2+}	Na^+	Zn^{2+}	Na^+	Zn^{2+}	Na^+	Zn^{2+}
Ny6/LDPE	15.8	12.1	26.1	20.8	24.8	25.7	13.0	23.0	17.3	22.2
Ny6/LDPE with 0.5 phr Na-EMAA	2.6	11.2	3.9	12.2	6.0	19.1	2.1	20.6	2.5	2.8
Ny6/LDPE with 1.5 phr Na-EMAA	1.7	9.5	2.5	10.5	2.7	18.1	2.3	20.2	1.7	2.0
Ny6/LDPE with 5 phr Na-EMAA	2.6	7.7	2.0	8.2	2.8	15.7	1.4	17.2	1.7	1.2
Ny6/ Na-EMAA	1.6	0.8	2.2	0.5	1.9	0.6	1.9	0.4	0.8	0.2

Table 2 Kinetic parameters of pure components and binary blends.

Pure component	Degradation temperature at 0.1 conversion (°C)	E_a (kJ/mol)	ln A (ln min^{-1})
Ny6	380.2	175.7	34.3
LDPE	311.8	122.0	27.1
Na-EMAA	354.6	102.5	21.7
Ny6/Na-EMAA blend ratio			
20/80	389.5	170.2	32.8
40/60	386.9	139.8	27.4
50/50	391.5	155.0	30.2
60/40	388.6	125.9	24.9
80/20	388.5	139.4	27.4
LDPE/Na-EMAA blend ratio			
20/80	369.0	154.4	31.0
40/60	360.6	255.0	50.4
50/50	352.5	243.5	48.8
60/40	345.7	226.8	46.2
80/20	335.7	189.8	39.4

Table 3 Kinetic parameters of Ny6/LDPE blends.

Na-EMAA content (phr)	Ny6/LDPE blend ratio	Degradation temperature at 0.1 conversion (°C)	E_a (kJ/mol)	ln A (ln min^{-1})
0	20/80	271.5	48.1	12.6
	40/60	292.7	71.9	17.2
	50/50	301.9	83.0	19.3
	60/40	318.9	70.1	16.2
	80/20	359.7	117.1	24.2
0.5	20/80	342.2	186.8	38.6
	40/60	355.9	285.4	56.7
	50/50	359.9	370.3	72.3
	60/40	358.1	232.0	46.2
	80/20	395.7	190.6	36.3
1.5	20/80	336.9	136.9	29.0
	40/60	385.0	476.0	89.0
	50/50	378.7	451.1	85.2
	60/40	365.3	444.4	85.9
	80/20	393.5	168.1	32.4
5.0	20/80	355.6	420.0	82.4
	40/60	349.2	322.5	64.3
	50/50	360.0	241.0	47.7
	60/40	354.1	252.2	50.3
	80/20	395.5	148.1	28.8

Table 4 Thermal properties of Ny6/Na-EMAA blends as a function of blend composition.

| Ny6/Na-EMAA | Exotherm | | | | | | Endotherm | | | | | | | | |
| | Na-EMAA | | | Ny6 | | | Na-EMAA | | | | Ny6 | | | | |
(% wt)	Onset (°C)	T_c (°C)	ΔH_c (J/g)	Onset (°C)	T_c (°C)	ΔH_c (J/g)	Onset (°C)	T_m (°C)	ΔH_m (J/g)	χ_c (%)	Onset (°C)	T_m (°C) γ	T_m (°C) α	ΔH_m (J/g)	χ_c (%)
0/100	68.0	62.3	58.7	-	-	-	84.0	95.2	41.1	14.6	-	-	-	-	-
20/80	71.6	63.0	38.4	176.2	167.0	5.7	85.3	95.9	29.1	12.9	207.6	-	218.9	11.6	30.5
40/60	72.6	63.5	30.4	188.0	184.5	9.6	85.1	96.5	22.5	13.3	199.0	213.7	222.4	24.7	32.5
50/50	75.4	67.6	32.8	185.5	180.8	28.0	85.1	96.0	18.7	13.3	203.3	209.8	218.7	27.2	28.6
60/40	76.2	68.8	22.8	183.9	179.3	39.3	87.9	96.0	15.5	13.8	200.6	208.4	216.0	33.9	29.7
80/20	83.0	72.5	8.9	185.5	181.1	49.2	89.2	95.9	8.1	14.3	203.3	210.2	219.0	43.9	28.9
100/0	-	-	-	191.4	187.1	67.0	-	-	-	-	207.3	215.7	222.0	56.6	29.8

Table 5 Thermal properties of LDPE/Na-EMAA blends as a function of blend composition.

| LDPE/Na-EMAA | Exotherm | | | | | | Endotherm | | | | | | | |
| | LDPE | | | Na-EMAA | | | LDPE | | | | Na-EMAA | | | |
(% wt)	Onset (°C)	T_c (°C)	ΔH_c (J/g)	Onset (°C)	T_c (°C)	ΔH_c (J/g)	Onset (°C)	T_m (°C)	ΔH_m (J/g)	χ_c (%)	Onset (°C)	T_m (°C)	ΔH_m (J/g)	χ_c (%)
0/100	-	-	-	68.0	62.3	58.7	-	-	-		84.0	95.2	41.1	14.6
20/80	77.5	74.5	0.5	69.8	65.5	22.9	101.0	106.0	3.4	6.0	81.0	95.2	14.5	6.4
40/60	93.0	89.6	21.0	70.5	65.8	29.9	101.1	106.4	10.3	9.1	84.0	95.5	11.7	6.9
50/50	92.3	88.8	29.2	69.6	65.5	21.1	101.0	105.5	13.9	9.9	84.8	95.0	5.5	3.9
60/40	92.2	89.0	35.7	69.7	65.6	16.0	97.4	104.4	18.2	10.7	88.9	92.2	4.5	4.0
80/20	92.1	89.1	47.4	96.4	65.0	6.5	99.7	104.4	27.2	12.1	86.5	93.7	0.8	1.3
100/0	92.3	88.8	58.8	-	-	-	100.2	105.2	48.9	17.3	-	-	-	-

Table 6 Thermal properties of Ny6/LDPE blends as a function of blend composition.

Ny6/LDPE (% wt)	Amount of Na-EMAA (phr)	Exotherm						Endotherm								
		Ny6			LDPE			Ny6					LDPE			
		Onset (°C)	T_c (°C)	ΔH_c (J/g)	Onset (°C)	T_c (°C)	ΔH_c (J/g)	Onset (°C)	T_m (°C) γ	α	ΔH_m (J/g)	χ_c (%)	Onset (°C)	T_m (°C)	ΔH_m (J/g)	χ_c (%)
Pure Ny6	0	191.4	187.1	67.0	-	-	-	208.2	215.7	222.0	56.6	29.8	-	-	-	-
Pure LDPE	0	-	-	-	92.3	88.8	58.8	-	-	-	-	-	100.2	105.2	48.9	17.3
20/80	0	187.8	183.0	11.3	95.5	91.6	44.1	208.9	211.7	220.0	10.1	26.6	102.3	108.0	37.8	16.8
	0.5	189.7	185.1	7.3	94.9	91.3	44.5	208.5	211.5	220.0	8.2	21.7	101.5	106.7	35.8	15.8
	1.5	188.7	182.6	5.4	95.3	91.5	45.5	207.4	210.2	219.5	8.7	23.2	101.7	107.4	34.6	15.3
	5.0	187.8	181.8	6.1	93.8	90.3	39.4	206.4	207.0	219.2	8.9	24.6	100.2	106.0	32.3	14.2
40/60	0	188.9	185.1	23.2	97.2	93.0	32.7	206.7	213.9	219.9	20.0	26.3	102.9	106.7	25.6	15.1
	0.5	189.6	185.0	24.8	94.4	90.3	41.2	209.1	212.2	220.5	21.8	28.8	101.9	107.4	27.2	16.0
	1.5	188.8	183.6	16.1	94.2	90.5	33.8	207.1	210.5	220.0	19.5	26.0	101.7	107.0	25.6	15.0
	5.0	188.4	183.8	15.1	93.1	89.6	27.4	206.7	210.2	219.2	17.6	24.3	99.9	105.0	23.5	13.5
50/50	0	189.4	184.5	32.1	96.9	92.5	22.2	206.3	216.4	221.4	28.3	29.8	100.9	107.5	20.0	14.2
	0.5	189.7	185.5	28.8	94.3	90.1	32.8	208.8	211.5	219.9	25.0	26.4	101.1	106.2	24.3	17.1
	1.5	191.2	186.5	46.5	97.7	92.0	11.0	206.9	213.9	221.0	39.1	25.9	100.0	105.9	11.6	20.1
	5.0	190.7	185.8	25.6	94.2	90.8	26.0	209.3	211.7	220.2	24.3	26.0	101.1	105.9	22.3	15.6
60/40	0	189.9	185.8	36.6	99.8	94.0	15.8	206.6	214.9	220.5	29.1	25.5	96.8	105.9	15.9	14.1
	0.5	189.7	185.8	34.9	94.2	90.3	22.7	209.8	212.9	220.9	31.1	27.4	101.3	106.5	20.1	17.6
	1.5	189.2	184.5	33.7	93.8	90.1	20.8	210.7	213.4	221.0	28.8	25.6	101.3	106.2	18.0	15.6
	5.0	190.3	186.6	27.6	93.3	90.3	16.2	206.4	212.4	220.5	28.8	26.5	99.1	103.7	15.4	12.7
80/20	0	191.8	188.3	48.0	98.6	93.6	6.9	210.1	-	220.0	34.4	22.6	100.4	106.9	8.3	14.6
	0.5	191.2	186.5	46.5	97.7	92.0	11.0	206.9	213.9	221.0	39.1	25.9	100.0	105.9	11.6	20.1
	1.5	187.8	184.3	45.9	96.9	91.6	9.4	213.6	216.4	222.9	36.8	24.6	100.6	106.7	10.8	18.1
	5.0	191.2	187.6	46.0	96.0	91.3	7.1	210.0	215.7	222.9	37.9	26.2	100.3	106.2	9.4	14.0